CFD Analysis of Wind Power Potential

Across Rooftop Gaps of Tall Buildings

by

Gargi Kailkhura

A Thesis Presented in Partial Fulfillment
of the Requirements for the Degree
Master of Science

Approved April 2017 by the
Graduate Supervisory Committee:

Huei-Ping Huang, Chair
Jagannathan Rajagopalan
Erica Forzani

ARIZONA STATE UNIVERSITY

May 2017

ABSTRACT

This study uses Computational Fluid Dynamics (CFD) modeling to analyze the dependence of wind power potential and turbulence intensity on aerodynamic design of a special type of building with a nuzzle-like gap at its rooftop. Numerical simulations using ANSYS Fluent are carried out to quantify the above-mentioned dependency due to three major geometric parameters of the building: (i) the height of the building, (ii) the depth of the roof-top gap, and (iii) the width of the roof-top gap. The height of the building is varied from 8 m to 24 m. Likewise, the gap depth is varied from 3 m to 5 m and the gap width from 2 m to 4 m. The aim of this entire research is to relate these geometric parameters of the building to the maximum value and the spatial pattern of wind power potential across the roof-top gap. These outcomes help guide the design of the roof-top geometry for wind power applications and determine the ideal position for mounting a micro wind turbine. From these outcomes, it is suggested that the wind power potential is greatly affected by the increasing gap width or gap depth. It, however, remains insensitive to the increasing building height, unlike turbulence intensity which increases with increasing building height. After performing a set of simulations with varying building geometry to quantify the wind power potential before the installation of a turbine, another set of simulations is conducted by installing a static turbine within the roof-top gap. The results from the latter are used to further adjust the estimate of wind power potential. Recommendations are made for future applications based on the findings from the numerical simulations.

DEDICATION

To my parents and my sister for making me what I am today.

ACKNOWLEDGMENTS

I am using this opportunity to thank each and every person who encouraged me in my endeavors to complete this research successfully. Firstly, I like to express my sincere gratitude to my Thesis Advisor, Dr. Huei-Ping Huang for his able guidance and support. I am glad to be his student, inspired by his undivided dedication and motivation to perfection and excellence.

I also thank Dr. Rajagopalan and Dr. Forzani, my committee members, for accepting my plea to be a part of my committee and bracing me up for completing my thesis smoothly.

And lastly, I thank my friends who have always been my pillar of strength throughout the completion of my research work.

TABLE OF CONTENTS

Page

LIST OF TABLES

Table Page

LIST OF FIGURES

Figure Page

Figure Page

CHAPTER 1

INTRODUCTION

Renewable energy in recent years is undergoing rapid developments as an alternative to fossil-fuel based energy. While many wind farms are built at locations away from cities, wind power potential in the urban landscape is being explored recently. Existing studies suggest a strong spatial variation of urban wind power potential, as exemplified by the contrast between windy spots above skyscrapers and wind shadows downstream of buildings. Moreover, the degree of acceleration over the rooftop depends on the detailed geometry of the building. Quantifications of these effects have important practical implications.

Given, this broad overview, the aerodynamic design of tall buildings strongly governs the effects of acceleration over the rooftop through the gap. The goodness of the design is measured by desired values of wind potential, acceleration ratio and turbulence intensity at the rooftop. A CFD numerical simulation with ANSYS Fluent 16.0, helps quantify the dependence of these measures using parametric analysis on geometric parameters – depth of gap, the width of the gap and building height. Yet, the validation of these CFD results becomes a little cumbersome as wind tunnel testing on real sized models is too difficult and costly to perform (Blocken et al. 2009).

The combined information of wind speed and turbulence intensity from numerical simulations provides a useful guidance for practical designs of green buildings suitable for

hosting rooftop micro wind turbines. The framework of numerical simulation developed in this work can be applied to other types of buildings for a more comprehensive assessment of wind power potential over the urban landscape.

Additionally, studying the simulations involving the presence of an installed static wind turbine incorporates more sharpness to the understanding of mounting wind turbines on a building rooftop gap. Conducting a comparative analysis of the above set-up with a case involving no wind turbine further incorporates more clarity to the principles of working of a wind turbine in exploiting wind energy in the urban landscape.

Nature of Wind Flow

Simulation of Wind flow around buildings in an urban environment is very important for tapping wind potential which can be utilized to meet the needs of the building. It, therefore, becomes essential to exploit this source of renewable energy for running smart sustainable cities (Silva et. Al 2015). Though wind energy holds an immense potential to be tapped, yet it hasn't been explored fully as of today. Wind flow over buildings largely depends on a lot of factors like meteorological effects, geographic setting, and geometry of the building (Ishugah et. Al 2014). The present study investigates the effect of two such co-factors namely inlet wind velocity profile and building aerodynamics on measurable quantities like gain in wind potential and turbulence intensity.

Wind Velocity Profile

The nature of wind flow or the profile of atmospheric boundary layer (ABL) is considered to follow the conservative 1/7th power law (Wikipedia: Wind Profile Law).

$$U(y) = u_0 . \left(\frac{y}{h}\right)^{\frac{1}{7}} \qquad (1)$$

where u_0 is the referential velocity (in m/s) at h altitude (in m) and U (in m/s) is the obtained velocity corresponding to y height (in m) (Figure 1).

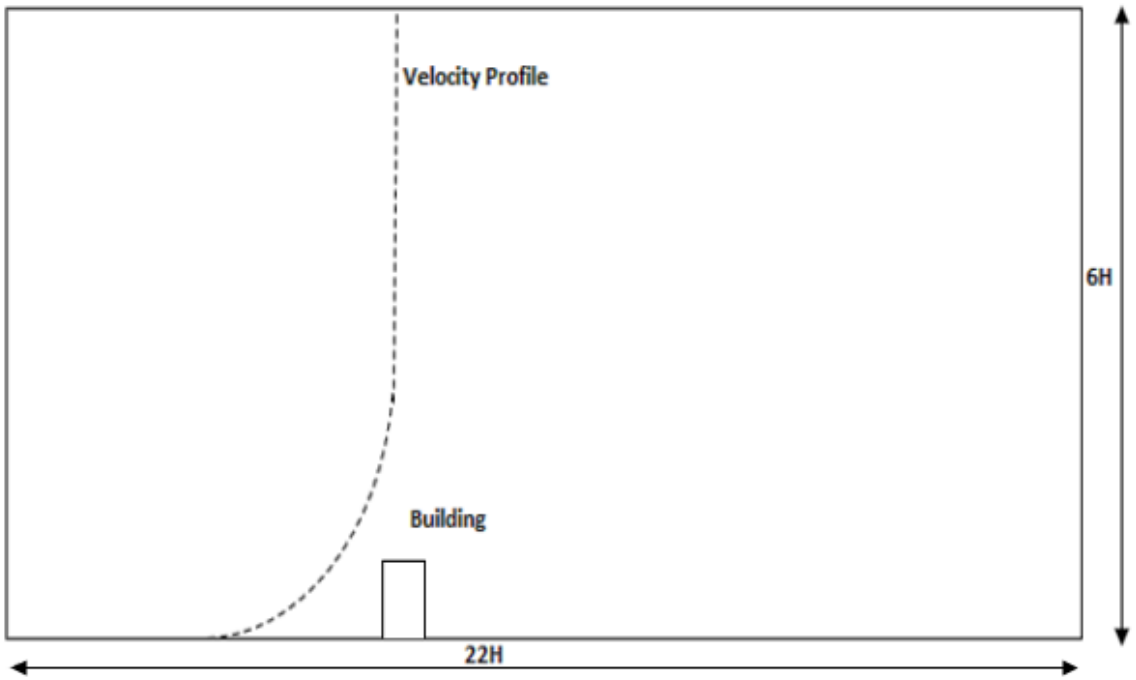

Figure 1. Representation of large CFD Domain-containing impending velocity striking the building

Two different cases of inlet velocity profiles are examined based on the referential inlet velocity (u_0) at CFD domain height (h). The main case however revolves around referential inlet velocity (u_0) taken as 18m/s at 144m (h) height. Further discussion is presented for u_0 = 10m/s at h= 144m.

Building Aerodynamic Design

The aerodynamics of roof design controls the airflow across the buildings. In this study, a special type of building is considered with a gap over the roof. Three geometrical parameters i.e. height of the building (H), the width of the gap (GW) and depth of the gap (GD) are selected to be varied in order to find the optimal location of a mounted wind turbine on such type of building rooftops (Figure 2). Parametric analysis is carried out to learn about the dependence of these geometric effects on acceleration ratio, wind potential, and turbulence intensity ratio due to wind flow across the urban landscape. These case studies are explained in detail in further.

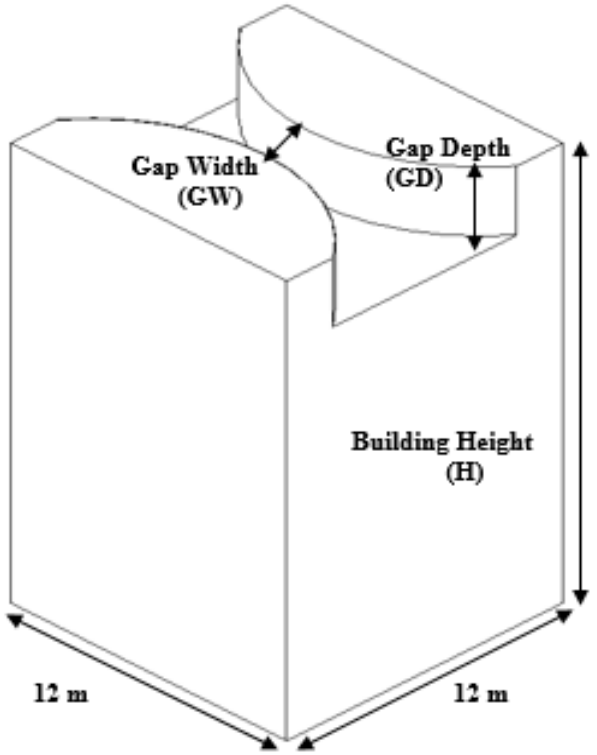

Figure 2. Geometric Parameters of Building as drawn in SOLIDEDGE.

CHAPTER 2

BACKGROUND LITERATURE

Study of building integrated micro-turbines isn't a new concept. The boon for this renewable energy, its low cost, and environment-friendly approach, has made it remain an expanding domain of interest for many researchers in the past. It was first previously explored by Abohela, Hamza, and Dudek. They focused on positioning and locating urban wind turbines by considering acceleration effect of different simple roof shapes like domed, gabled, vaulted and pyramidal, as well as different building heights (Abohela et. al 2012).

An equilibrium ABL was modeled in a 3D CFD domain with dimensions depending upon the building height as 22H x 6H x 6.6H, using CFD Code Fluent 12.1. The boundary conditions used a User Defined Function (UDF) for inlet velocity. The results described by them explained the distribution of wind flow across the building drawn as a cube. The wind separation into four different directions over the building happened at the point of maximum pressure. In the windward direction of the cube, a horseshoe vortex formation was observed. This wind flow separated and reattached in the leeward direction of the building resulting in the formation of recirculation zones.

Their research concluded that in such a CFD modeling of the building, there was an acceleration in the velocity near the building and increase in turbulence intensity around the vicinity of the building. By conducting numerical modeling for different building heights, they noted a relationship between the building height, turbulence intensity and

acceleration ratio. The turbulence intensity increased with increase in building height while acceleration ratio remained almost consistent with the increase in height. In the present study, these parameters are therefore considered as the governing factors for ideally locating the micro wind-turbine at the building rooftop.

Furthermore, optimizing the wind turbine performance is the most important concern regarding the installation of Building-Integrated Wind Turbines (BIWT). Many such research works have contributed greatly in studying the simulation of environmental flow over urban landscape for renewable energy applications. One such work done by Sari and Cho shared a similar objective of performing comparative analysis but from differently designed rooftop models to evaluate the maximum wind speed at the rooftop for mounting wind-turbine (Sari and Cho 2014). They incorporated Power Law Formula for incoming wind velocity profile in ABL. CFD commercial code Fluent 6.2.16 was used for numerical modeling with results showing Acceleration Ratio in the range of 1.4 and the best horizontal position for the turbine in the range of 2m – 5m high from the rooftop base for the optimal design. They also validated their results by carrying wind tunnel experiments and tested their turbine model in Seoul, South Korea. Thus, they optimized wind turbine performance by checking for increasing wind speed with modifying building rooftops.

Their building designs were so inspirational that the present research uses it in designing the current building model. There are sincere efforts put forward to improve the wind energy exploitation to meet the energy demand in turbulent urban wind environment. This

is done by using horizontal-axis wind turbines (HAWTs) and vertically axis wind turbines (VAWTs). One such illustration was provided by Ishugah, Wang, and Kiplagat.

They studied the wind flow characteristics in an urban environment by gathering data for average wind velocity and turbulence intensity at different heights for over a month for Masdar city, UAE (Ishugah et. Al 2014). A particular wind turbine was then selected after analyzing the processed data. Different orientations of wind turbines like HAWTs and VAWTs are examined so as to know which conditions deliver the best optimum results. They also considered the technique of using micro-wind turbines mounted on new and existing homes. Several examples were cited using roof mounted wind turbines integrated building structures having applications at the airport, towers, and urban highway. Thus, they analyzed the actual collected data and proposed new solutions for the application of wind energy technology in urban areas, considering factors like population, resources, affordability and security.

Learning about new technologies on tapping maximum wind potential is the need of the hour. And so more research is going on in this field.

Lu and Ip led a research on the feasibility of wind power utilization in local urban areas and on how to compute wind power more effectively (Lu and Ip 2007). Their conclusion proposed the idea of the concentration effect of buildings and height of buildings in influencing wind potential at building rooftops. They CFD modeled annual wind flows over buildings to analyze, locate and design the turbines in and around the buildings. They further developed strategies on how to develop wind power by utilizing building

parameters like optimal shapes (concave arc, convex arc, hemisphere etc.) of building roofs.

Though such research works have been helping in analyzing wind flow over different building rooftops but never did any of the works focused on studying the effects of building geometrical parameters like building height or dimensions of the rooftop gap of a particular building design on wind flow. Thus, the present investigation majorly focuses on optimizing different and innovative effects that can be introduced in a specific building with rooftop gap, for mounting micro-wind turbines on it.

CHAPTER 3

METHODOLOGY

Modeling Parameters

As discussed, different cases are run for carrying out the parametric analysis. The model is modified by adapting Reynold Scaling with the length being scaled to 1/4th of the original length while velocity is being scaled to 4 times the real value. Results obtained later are again brought down to the actual values.

$$Re = \frac{\rho * v * d}{\mu} = \frac{\rho * (4 * v) * (d/4)}{\mu} \qquad (2)$$

The domain of *22H x 6H x 6.6H* (Abohela et. al 2012) is selected considering the scaled lengths, resulting in a blockage of 1%, with respect to the building height (H). Wind flow length, domain height, and domain thickness are represented by 22H, 6H, and 6.6H respectively. This domain size is taken with respect to the highest building height (H=24m). Roof shapes have an actual scale of the base area of *12m x 12m*. In the present study, five different building heights namely H = 8m, 12m, 16m, 20m, and 24m have been taken into account. A parameter like a gap depth is varied as 3m, 4m, and 5m while gap width is varied as 2m and 4m.

The ABL profile is governed by the 1/7th power law as stated earlier (1). The velocity of wind flow (v) across the building is vital in determining the wind potential (P), turbulence intensity ratio and the optimal location for mounting wind turbine in such conditions. Acceleration Ratio (AR) is an important quantity in determining Wind Potential Gain (ΔW) and Wind Potential Gain Fraction ($\Delta W/W$). AR is defined as the ratio of wind speed in

presence of building to its counterpart in the absence of the building, at the same position. This correlation is the correct measure in learning about the effective wind flow across the turbine.

$$AR = \frac{v_b}{v_{nb}} \qquad (3)$$

where,

v_b = Velocity of wind with building in domain (m/s)

v_{nb} = Velocity of wind without building in domain (m/s)

The key quantity, however, is wind power potential which is obtained from the following formula:

$$P_{turbine} = \frac{1}{2} * \rho * C_p * A * v^3 \qquad (4)$$

where

$P_{turbine}$ = Wind power potential (W)

ρ = Wind flow density (kg/m^3)

C_p= Coefficient of Performance

A = Swept area of turbine blades (m^2)

v = Free wind speed (m/s)

Turbulence Intensity, another quantifiable parameter is defined as the ratio of Root-Mean Square of turbulent velocity fluctuation (u') to the Mean velocity fluctuations (U) (Turbulence Intensity Application Note TSI-141, 2012).

$$T.I = \frac{u'}{U}$$

Wind Turbine Selection

From the above equation, it is inferred that the power increases with the cube of the wind and the plot obtained between them is called as the power curve. This curve is used for getting an insight into the selection of wind turbine (Simic et. al 2012). After some cut-off velocity, the power remains constant and achieves saturation. The narrowest gap between the airfoil lobes of the roof structure is observed to be the optimal location for a wind turbine as seen after running the CFD simulations. And so, the ultimate choice of a wind turbine is determined by examining the data pertaining to turbine size and the effective power output. For an ease of understanding, the wind turbine model *Windside WS-30 corr.* with a power density of $1kW/m^2$, is selected such that it obeys the power curve hypothetically (Simic et. Al 2012).

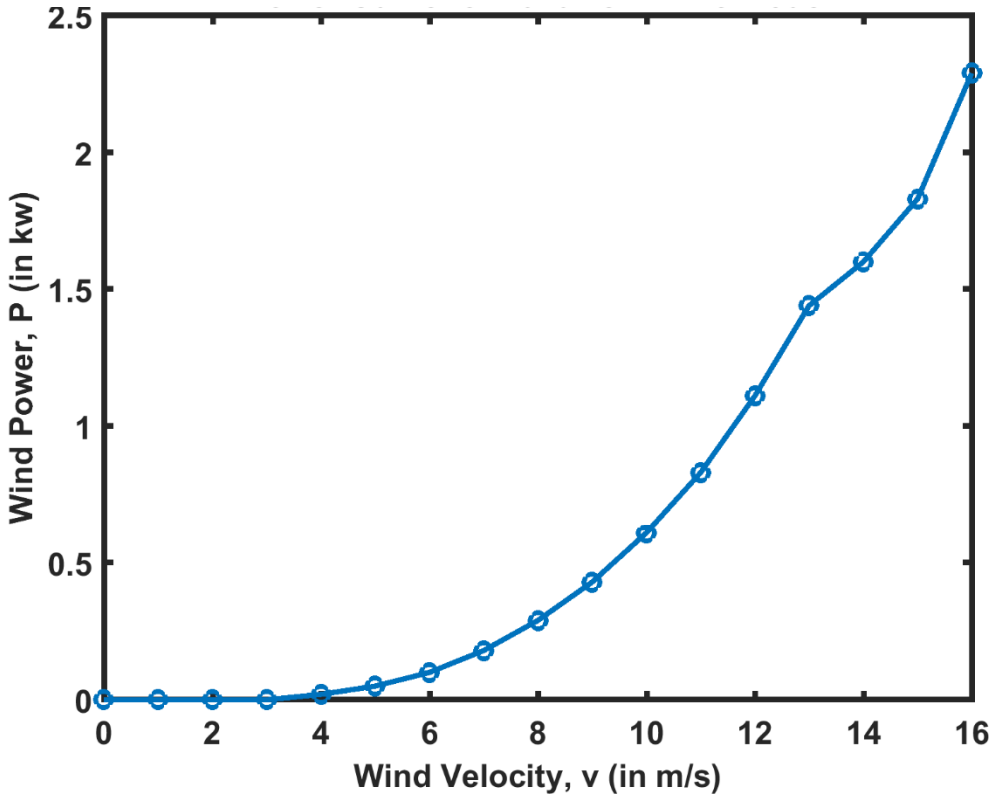

Figure 3: Power Curve for Turbine Windside WS-30 corr. (Simic et. al 2012).

For simplified calculations, a different variable, C, is introduced such that:

$$P_{turbine} = C * v^3 \qquad (5)$$

The above power curve is plotted by taking data from the paper (Simic et. al 2012) where velocity varies from 4m/s to 16 m/s. But, in our case, the velocity reaches up to 18m/s. And so, the curve is extended and assumed to follow the cubic nature up to 18m/s.

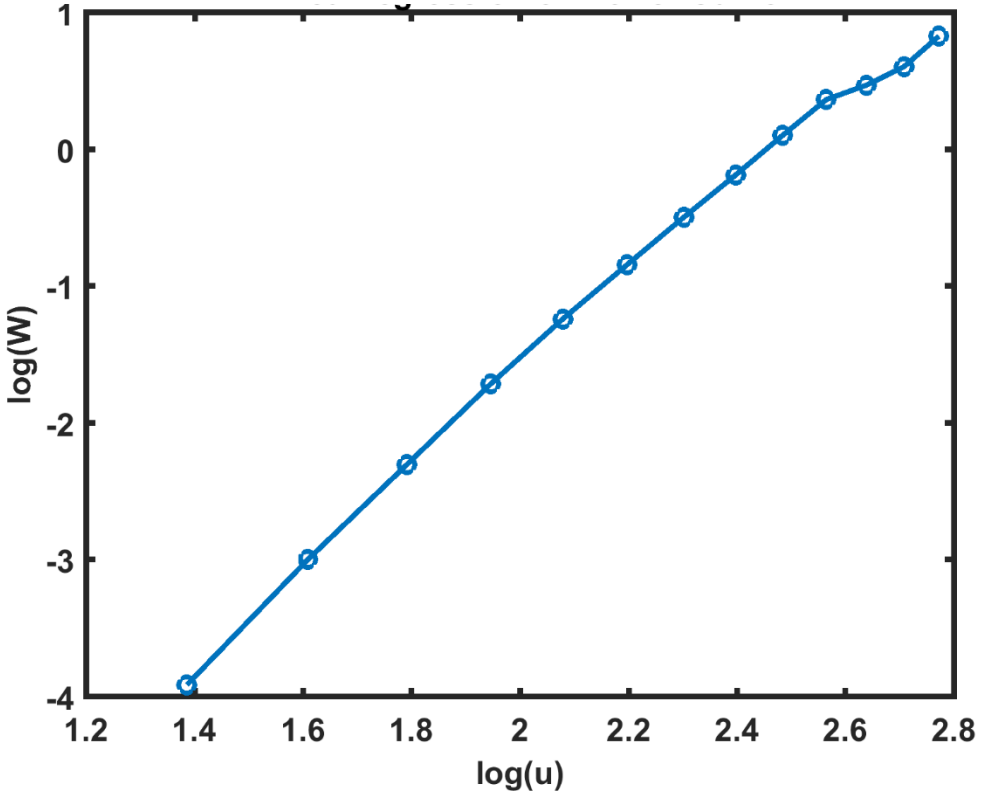

Figure 4: Linear Regression on the above Power Curve

The value of C, however, is computed from linear regression and available turbine data, provided P is in kW and v is in m/s. From the above regression graph plotted from turbine data available in the paper reference (Simic et. al 2012),

$$\log(w) = -8.413 + 3.3952 * \log(u) \qquad (6)$$

And we know,

$$W = C * u^3$$

$$\log(W) = \log(C) + 3 * \log(u) \qquad (7)$$

$$\log(C) = \log(W) - 3 * \log(u)$$

From (6), approximating 3.3952 as 3, and comparing it with (7).

And from Eq.3, averaging values of log(C) obtained by plugging the velocity and power data from power curve, log(C) is found out to be -7.535 or C = 0.000534.

Thus, the formula can be redefined as:

$$W = C * u^3$$

where C = 0.000534, provided u is in m/s and W is in kW.

Thereafter, further calculations on the gain in wind power potential (ΔW), due to the presence of the building are carried out by the following adopted methodology.

$$W = C * {v_{nb}}^3$$

$$W' = C * {v_b}^3$$

$$\Delta W = W' - W = C * ({v_b}^3 - {v_{nb}}^3) = C * {v_{nb}}^3 * \left(\frac{{v_b}^3}{{v_{nb}}^3} - 1\right)$$

$$= C * {v_{nb}}^3 * (AR^3 - 1) \qquad (6)$$

Besides wind power potential, turbulence intensity is another important quantity to be considered for mounting wind turbines. Higher turbulence intensity is a threat to the stability of wind turbines on rooftops (Abohela et. al 2012). And so lesser the turbulence intensity, better the safety and steadiness of the turbine.

CHAPTER 4

CFD NUMERICAL SIMULATIONS

Main Simulation

CFD numerical analysis is implemented in the present study for investigating the velocity of wind flow across the buildings. ANSYS Fluent 16.0 is used as the CFD solver in this analysis. With the Reynold scaling factor of 4, the domain of *528m X 144m X 158.4m* is scaled down to *132m X 36m X 39.6m* (Figure 3) for practicality and the velocity is scaled up from 18 m/s to 72m/s. The base area of the building is also scaled down to *3m X 3m*. And this domain size is taken to be the same for all the numerical simulations so as to provide a justified comparison among the different case studies. The leading edge of the building is located at a distance of *8.3 H* from the velocity inlet side.

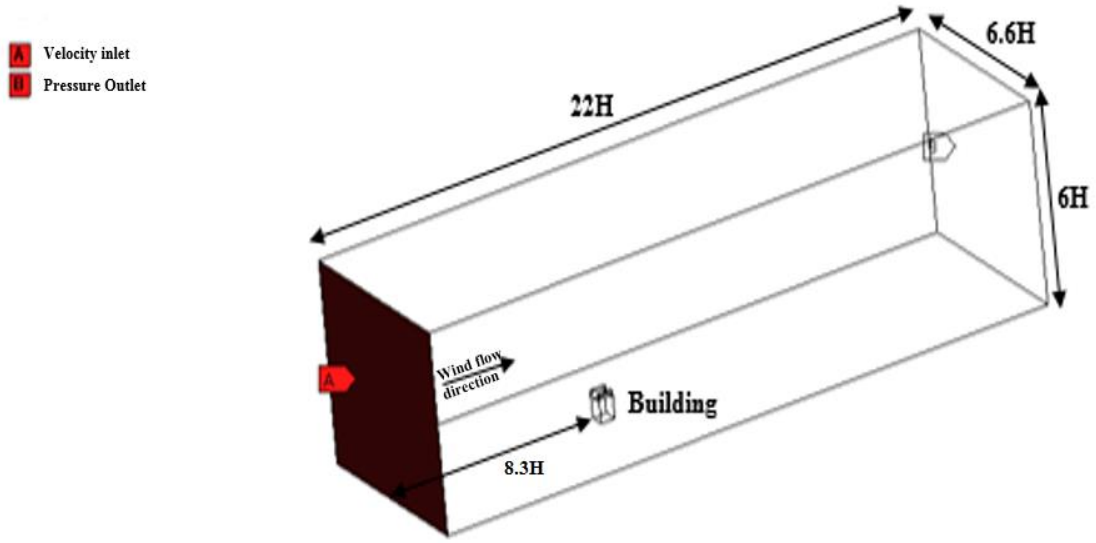

Figure 5: Domain as seen in ANSYS Fluent 16.0

After geometrically designing the prototype, meshing is performed on the entire model (Figure 4). Imposing medium relevance center mesh and a very fine element size of 0.25m, around 1 to 2 million nodes are obtained for such a large domain.

Details of "Mesh"

Display	
Display Style	Body Color
Defaults	
Physics Preference	CFD
Solver Preference	Fluent
Relevance	0
Sizing	
Use Advanced Si...	Off
Relevance Center	Medium
Element Size	0.250 m
Initial Size Seed	Active Assembly
Smoothing	Medium
Transition	Slow
Span Angle Center	Fine
Minimum Edge L...	0.50 m
Inflation	
Assembly Meshing	
Patch Conforming Options	
Patch Independent Options	
Advanced	
Defeaturing	
Statistics	
Nodes	1736172
Elements	9591975
Mesh Metric	None

Figure 6: Mesh Statistics obtained in ANSYS Fluent

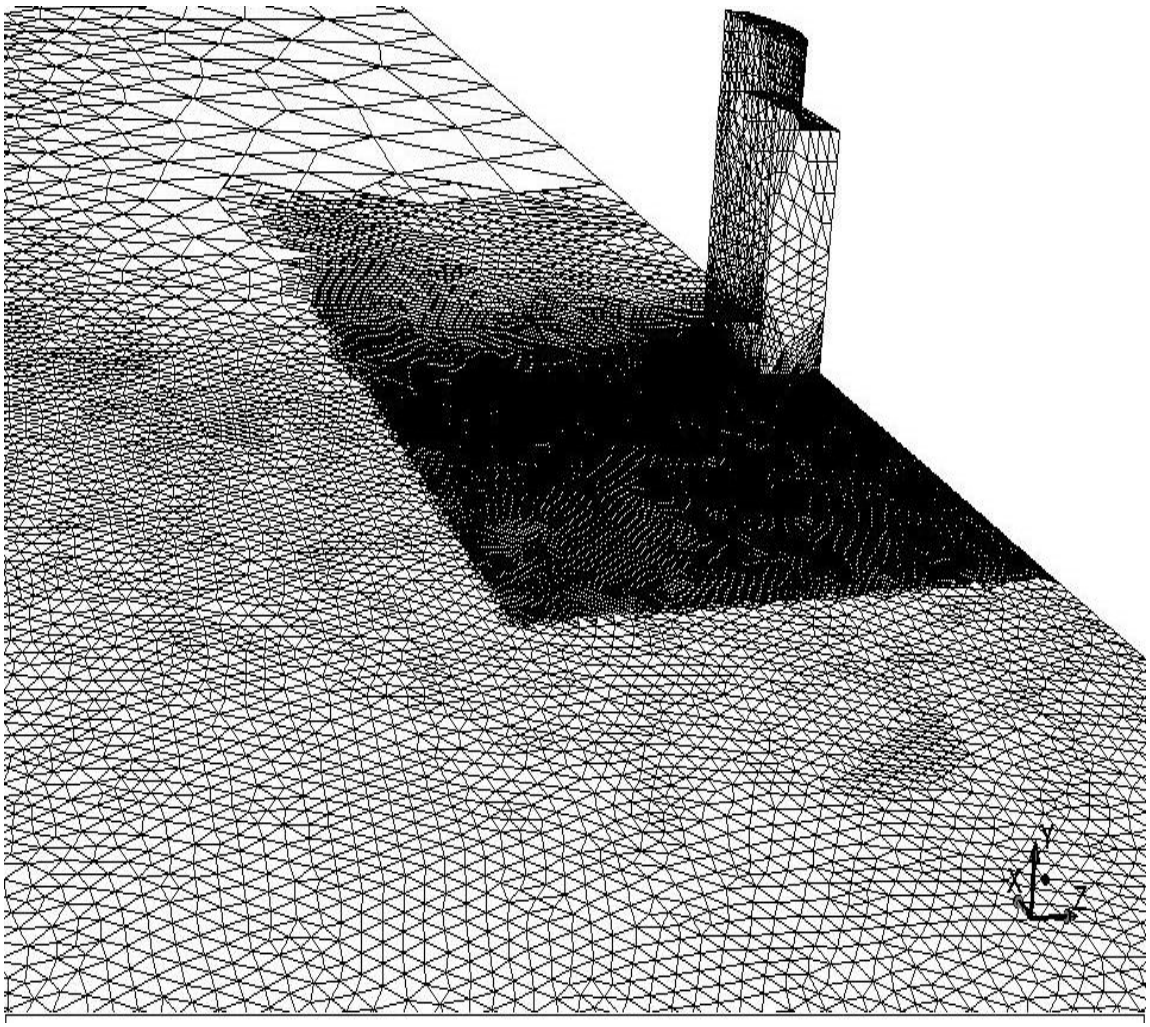

Figure 7: Meshing containing regional adaption around the building

The meshed model is then ready for a steady-state setup where pressure based solver is used. To account for turbulence intensity, k-ε turbulence model type is employed. Boundary conditions are selected as velocity inlet, pressure outlet, symmetry, and walls.

The boundary from which the wind flow originates is termed as the velocity inlet. A UDF is developed containing the inlet velocity profile and an added custom defined function. The outlet of the domain signifying the end of the wind flow is called as the pressure outlet.

Symmetry is enforced upon the side faces and the top face, assuming the nature of outside flow as same as that of the inside flow of the domain. The bottom face, as well as the building extrusion faces, are assumed as stationary walls. SIMPLEC scheme, limited by pressure-velocity coupling, is adopted for speeding up the convergence in this complicated turbulent flow model. Spatial discretization is taken as the Second order in Pressure and Momentum; and First order in Turbulent Kinetic Energy and Turbulent Dissipation Rate. Convergence criteria are set up by monitoring residuals of velocity in the order of 10^{-5} while continuity and turbulence parameters (k, ε) in the order of 10^{-3}. For getting more accurate results, region adaption is applied near the areas surrounding the building (Figure 4).

To save computational time, the simulations are run with parallel processing of 6 core processors. Solutions are then observed to converge within 800-1000 iterations. Results obtained are then proceeded for post-processing. Post-processing involves extracting velocity and turbulence intensity data along vertical lines placed 0.375m (scaled) apart across the building rooftop, starting from the gap depth till the height of 12m from the rooftop (Figure 5).

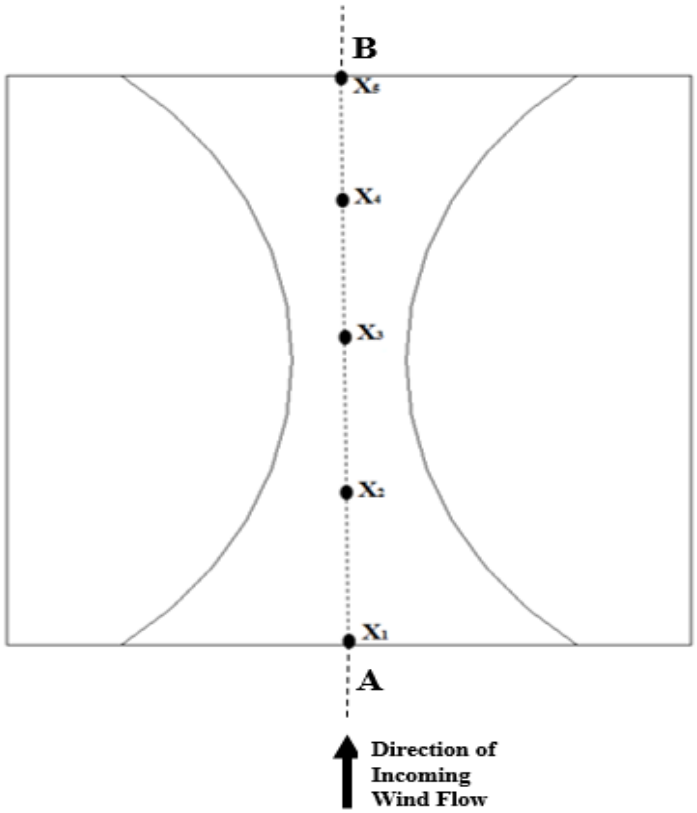

Figure 8: Extracting data along the vertical lines drawn at X_1, X_2, X_3, X_4 and X_5 across the building rooftop gap.

Simulations in Presence of Static Turbine

For finding the optimum position for mounting wind-turbine, maximum wind potential and minimal turbulence intensity values are desired. This post-processing process as mentioned above is used for finding such optimum conditions for positioning the turbine. It eventually helps in determining the position of micro-wind-turbine to be mounted on the building rooftop. The wind turbine so chose, *Windside WS-30 corr* which hypothetically follows the power curve, is thus apt for the present study.

To run this numerical model, a separate run of computational simulations of the previous domain but in the presence of micro-wind turbine, is considered. The CFD domain i.e. *120m X 20m X 36m* is drawn in ANSYS Workbench, in true scale, excluding Reynold Scaling. Three blades are drawn around 1m long, with a thickness of 0.05m each and at a height of 2.5m from the rooftop base.

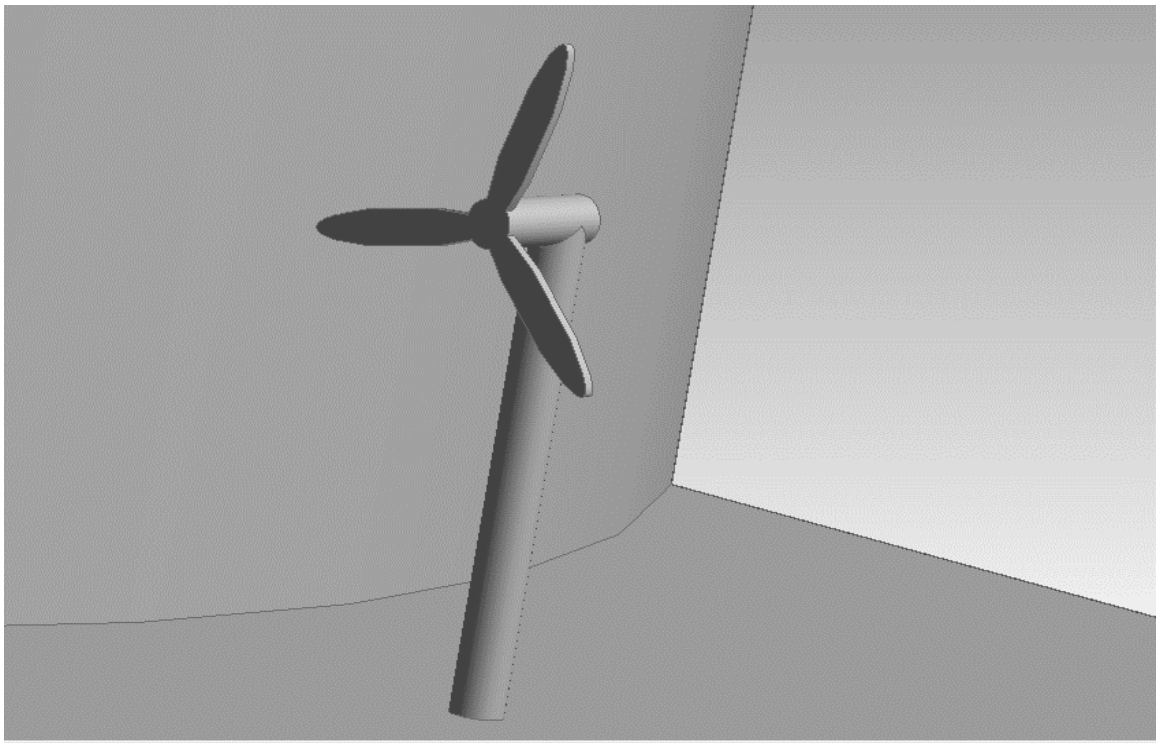

Figure 9: Wind Turbine as drawn in ANSYS Workbench

This static wind-turbine model is then meshed finely containing around 1 million nodes and a 1 scale refinement on the turbine.

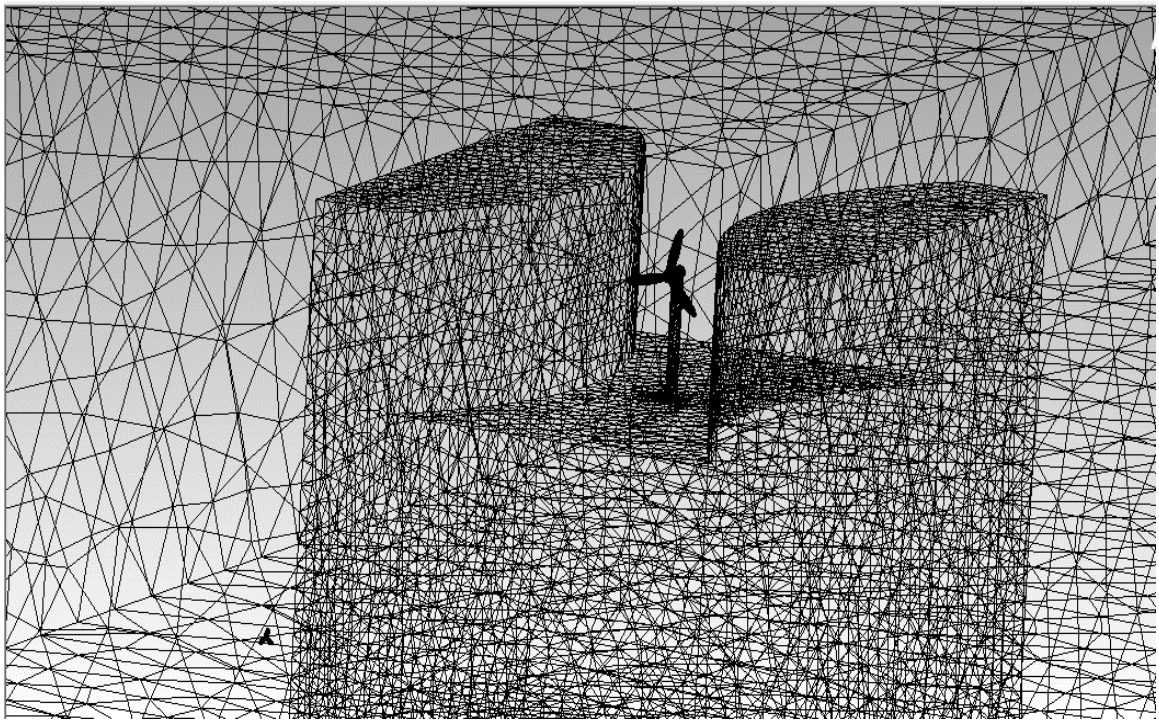

Figure 10: Meshing as performed on the domain containing wind turbine

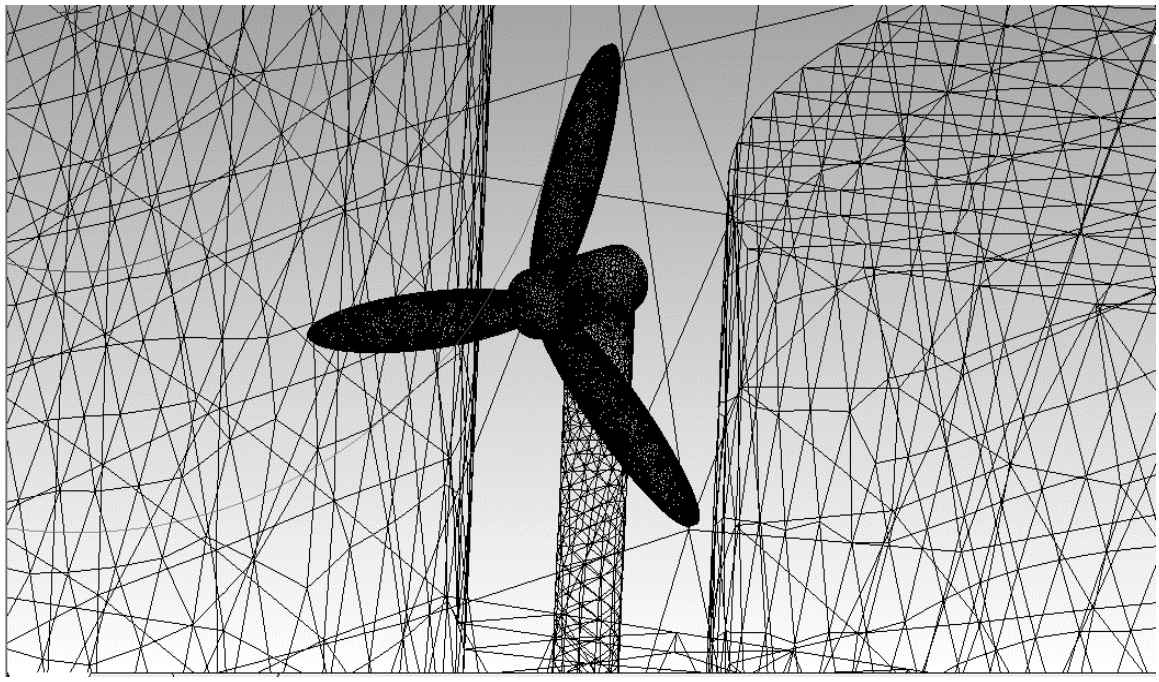

Figure 11: Mesh Refinement done on Wind Turbine (Zoomed Image)

After obtaining the meshed model containing wind turbine, it is finally sent for Numerical Solution where inlet velocity is assumed as constant as 18m/s. Since the domain focuses on the zoomed building region, the velocity is assumed to be same in that region. The other boundary conditions are taken as same as previously i.e. inlet velocity, pressure outlet, symmetry and walls except that walls now also include the turbine extrusions. The model is thus set up so as to study the behavior of static turbine when it is just kept at the building rooftop gap. The turbine is placed as stationary and is ready to rotate, facing the winds from the velocity inlet boundary side. In this case, after 600-800 iterations, the CFD model converges to get the desired results, which are discussed later in this research. Along with velocity and turbulence intensity contour plots, drag and lift forces so generated due to the static turbine are also determined.

CHAPTER 5

RESULTS AND DISCUSSION

Elementary Results

The flow of velocity across buildings is studied in detail using contour plots obtained on the rooftop plane and on the midplane of the domain thickness (6.6H). Velocity contour plots are observed to attain maxima around the rooftop gap as shown in the figure. A recirculation zone is also spotted just behind the building. This behavior can be explained due to variance in pressure and turbulence across the regions surrounding the building. There is high pressure in the region at the start of the building edge which eventually reduces and becomes negative as the flow reaches the rooftop. It further reduces to a minimum surrounded by low-pressure regions behind the building, in an undirected manner. This can be attributed to the turbulence generated in that region producing vortices and hence the backflow. So, the cumulative effect of pressure and turbulence results in such velocity flow pattern which separates on facing the windward side of building edge and then re-attaches again on the leeward side of the building. Since there are separation and reattachment of the flow, formations of recirculation zones are pretty evident to observe (Abohela et. al 2012).

From the contour plot on the rooftop plane, a very clear result is achieved with the velocity increasing rapidly as it enters the nuzzle-like narrow gap between the airfoil shaped lobes and eventually reaches its maxima around the center of the gap. Some part of the inflow gets deflected by the airfoil structure. Parameters like gap depth, gap width, and building height are varied in order to study their effects on getting maximum velocity magnitude.

All in all, the velocity magnitude is majorly determined by the aerodynamic shape of the airfoil like structures on the rooftop. All the plots shown below are pertaining to the case of H=20m, GW=4m, and GD=5m.

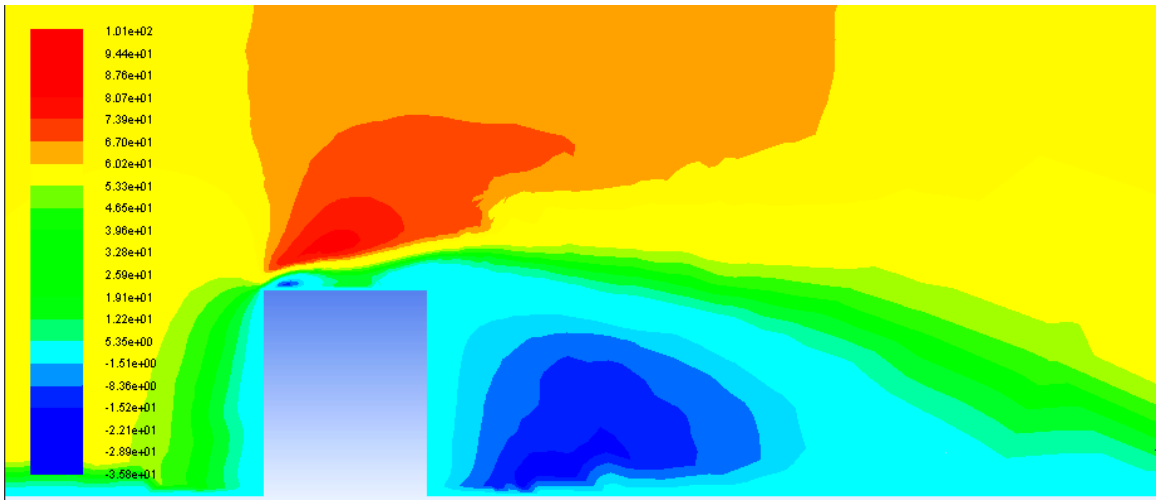

Figure 12: Velocity Contour Plot at mid-plane of domain thickness

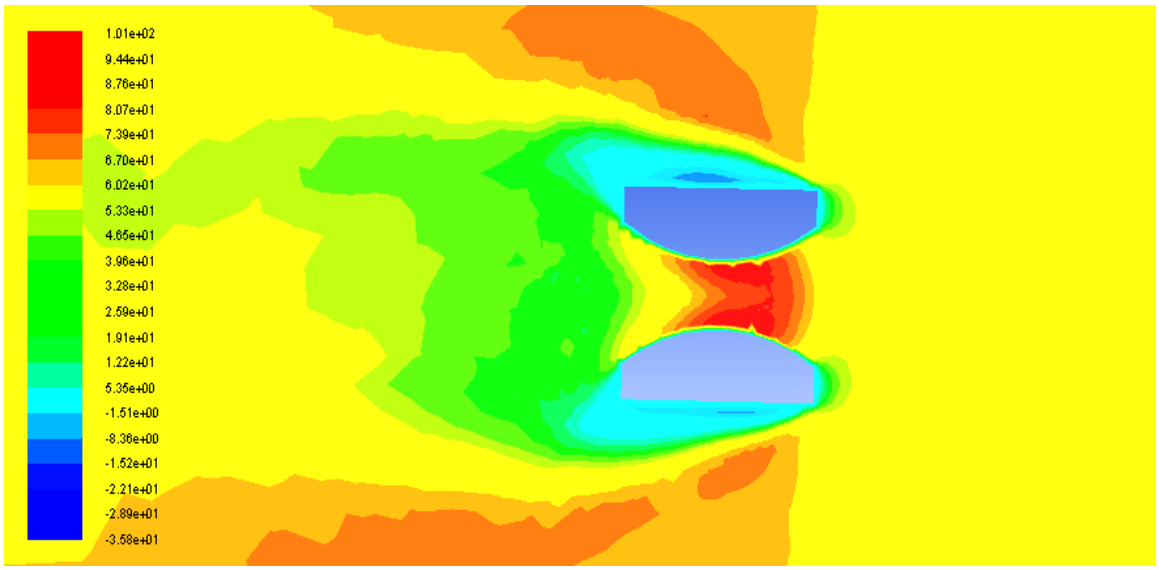

Figure 13: Velocity Contour Plot just above rooftop plane

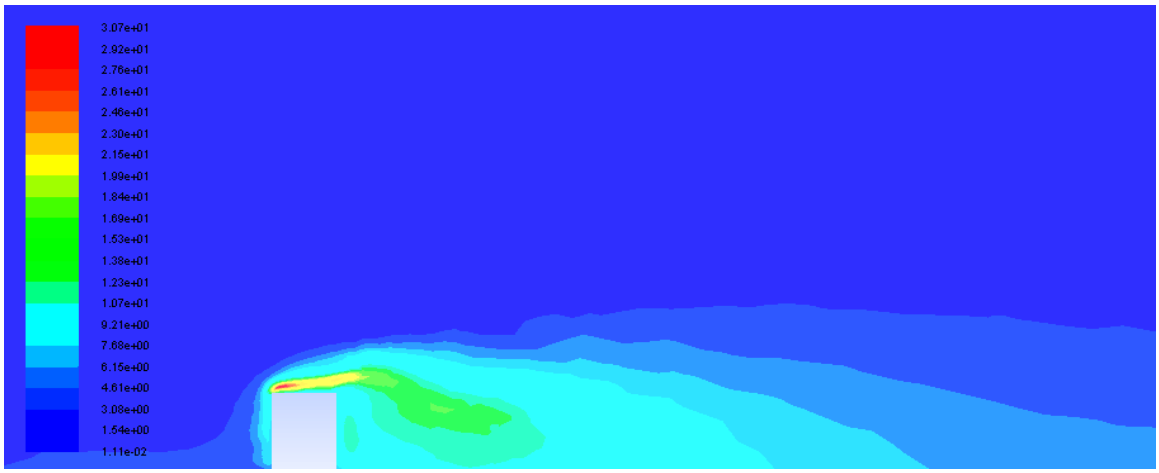

Figure 14: Turbulence Intensity Contour Plot at mid-plane of domain thickness

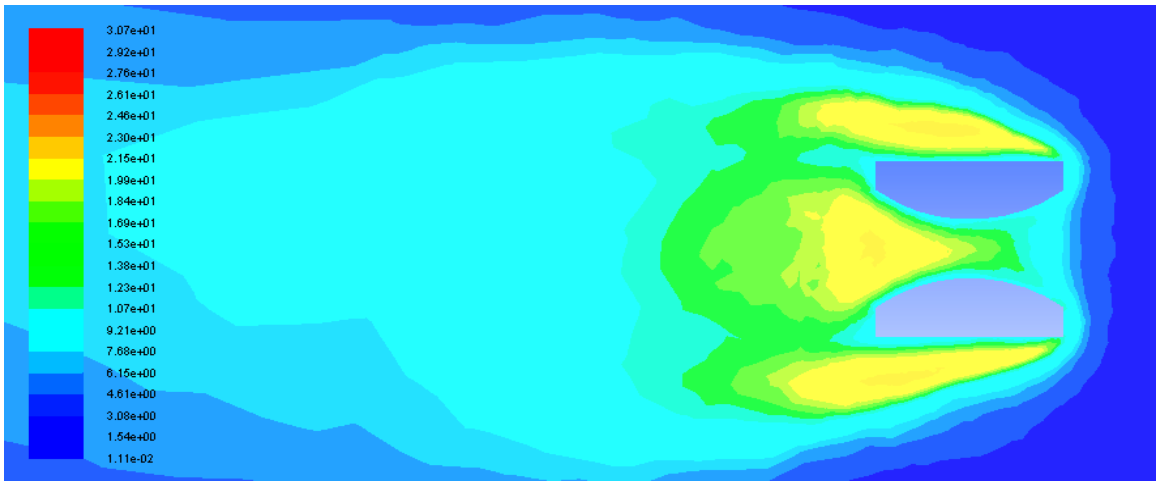

Figure 15: Turbulence Intensity Contour Plot just above the rooftop plane

Similarly, the effect of turbulence intensity due to various building parameters is studied in detail. The results, however, seem a little mysterious and obscure to infer. For the contour plot at mid-plane of the domain thickness, turbulence intensity is seen to rise gradually as it flows through the building with very sudden increase near the recirculation zone. The building acts as an obstruction to the wind flowing in a largely closed domain. Recirculation zone contains high turbulence intensity due to vortices formation resulting

in backflow of air. From the contour plot of Turbulence Intensity on the rooftop plane, it is seen that as the wind flows past the two lobes, the turbulence intensity increases across the edges on the sides. This can also be perceived as the lobes acting like an obstruction against the flow of wind moving in a largely closed domain. One common thing that can be inferred from both the contour plots is that turbulence intensity is high only behind the building and so mounting of the turbine inside the rooftop gap appears alright. From the background literature, minimal turbulence intensity is desired, so as to avoid instability and unsteadiness of the wind turbine. All in all, the mounting of micro wind turbine inside the rooftop gap poses no threat in terms of turbulence intensity factor.

In general, the numerical simulations so obtained are observed to be in agreement with the Background Literature. A typical acceleration ratio plot and turbulence intensity ratio plot is shown below. It validates with the results shown by Abohela (Abohela et al 2012).

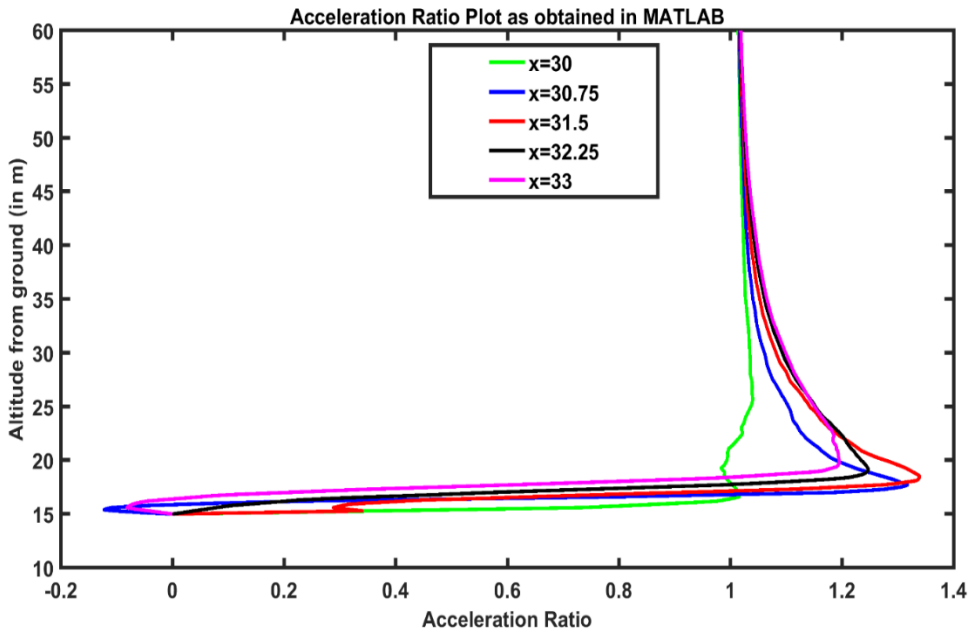

Figure 16: Acceleration Ratio as plotted in MATLAB

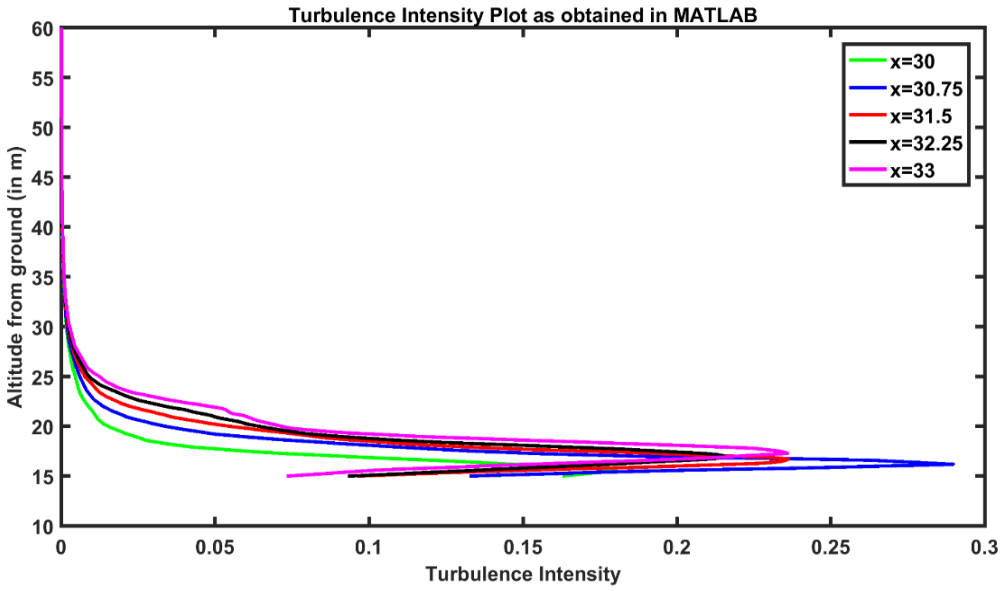

Figure 17: Turbulence Intensity Plot as obtained in MATLAB

There are data sets showing negative acceleration ratio as well. These values represent the wind velocity in the region where building is already present and hence wind flow cannot be accounted properly. This reason accounts for the non-positive wind velocity values corresponding to that height.

Parametric Analysis

The main focus of the study is to investigate the effects of different parameters like Building Height (H), Gap Depth (GD) and Gap Width (GW) on output parameters like Acceleration Ratio, Wind Power Potential Gain, and Turbulence Intensity. The cases the study focusses on are based on impending velocity governed from 1/7th power law Eq. (1) with 18m/s at 144m.

Case 1: H = 8m

- GD: 3m, 4m, and 5m
- GW: 2m and 4m

Case 2: H = 12m

- GD: 3m, 4m, and 5m
- GW: 2m and 4m

Case 3: H = 16m

- GD: 3m, 4m, and 5m
- GW: 2m and 4m

Case 4: H = 20m

- GD: 3m, 4m, and 5m
- GW: 2m and 4m

Case 5: H = 24m

- GD: 3m, 4m, and 5m
- GW: 2m and 4m

Running numerical simulations using ANSYS 16.0 for all these cases, the respective data for velocity and turbulence intensity are extracted as done previously along the vertical lines at x_1, x_2, x_3, x_4, and x_5. It is then processed using MATLAB Coding. The results so generated are expressed as:

Dependence of Acceleration Ratio on Design Parameters

Two different plots representing cases of GW = 4m and GW = 2m are considered for penning down the effect of acceleration ratio on gap depths corresponding to different heights. Both display same trend with acceleration ratio, corresponding to respective building heights but increasing with gap depth. These acceleration ratios also increase from GW = 4m to GW = 2m which implies that narrowing the gap makes the structure aerodynamically beneficial for high wind speed flow. Also, it is relatively insensitive to the height of the building. For Example, acceleration ratio in H = 8m case is nearly the same or greater than that of H = 20m case. This is because H = 8m with a GD = 4m or GD = 5m makes the building almost half or more than half as hollow. Since the aerodynamic shape of the whole building changes, the trend is nonspecific.

Table 1: Variation of Acceleration Ratio with Design Parameters

		H = 8m	H = 12m	H = 16m	H = 20m	H = 24m
	GD = 3m	1.2057	1.1895	1.1779	1.2277	1.214
GW = 4m	GD = 4m	1.2305	1.2717	1.2408	1.2479	1.2633
	GD = 5m	1.3131	1.3113	1.3233	1.2961	1.2998
		H = 8m	H = 12m	H = 16m	H = 20m	H = 24m

	GD = 3m	1.3398	1.2311	1.2479	1.2442	1.2412
GW = 2m	GD = 4m	1.6126	1.5292	1.4673	1.4675	1.4832
	GD = 5m	1.8848	1.7133	1.691	1.6995	1.6667

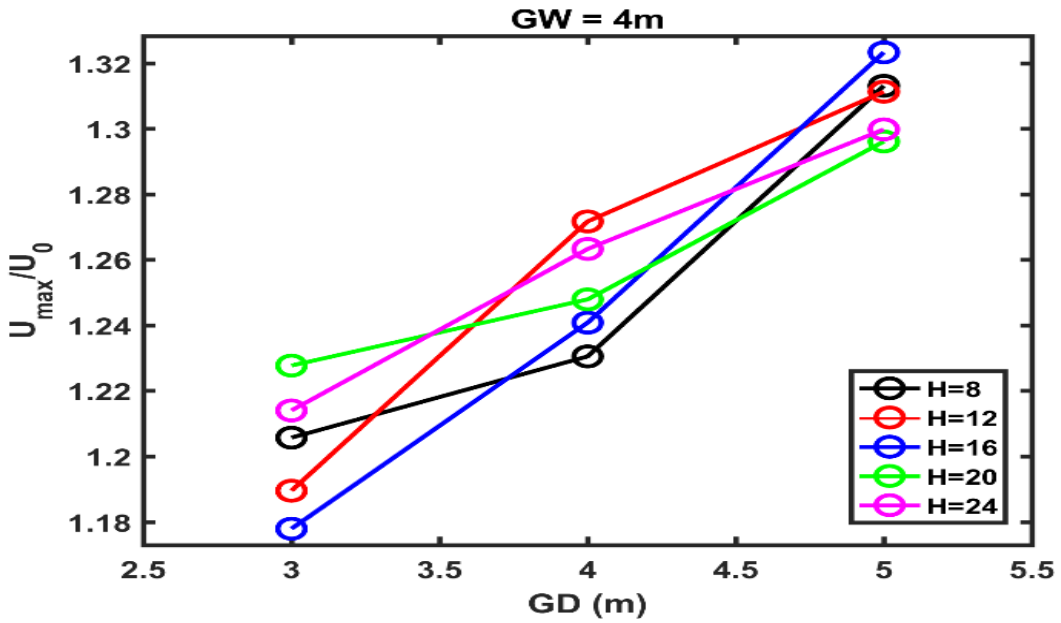

Figure 18: Line Plot of AR on GD for GW = 4m case, as obtained in MATLAB

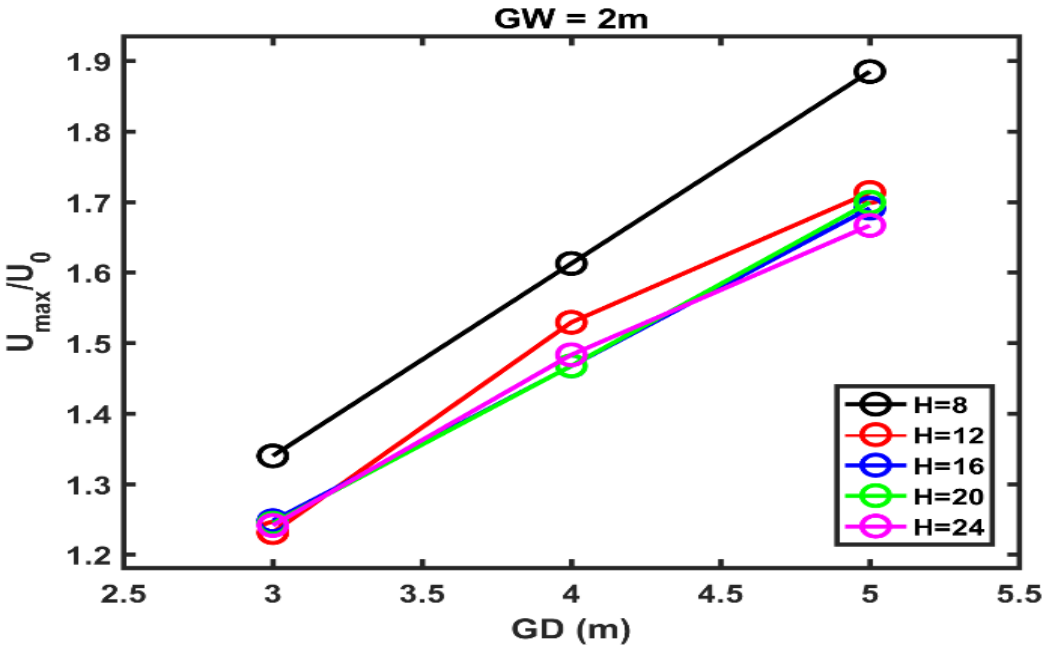

Figure 19: Line Plot of AR on GD for GW = 2m case, as obtained in MATLAB

Dependence of Gain in Wind Potential on Gap Depths

The trend of wind potential gain (ΔW) follows kind of similar nature as the previous trend as ΔW is directly proportional to the cube of AR. All in all, it ranges from 2.1413 kW to 12.6364 kW and so the wind turbine, if placed, can generate power lying in the above-mentioned range. It also increases with increase in Gap Depth and with a decrease in Gap width. Again, its trend isn't that clear with building height as it first increases, then decreases and then increases. The reasoning for H = 8m case as explained before holds true here also.

Table 2: Variation of Wind Potential with Design Parameters

		H = 8m	H = 12m	H = 16m	H = 20m	H = 24m
	GD = 3m	2.3374 kW	2.1413 kW	1.9872 kW	2.6631 kW	2.4703 kW
GW = 4m	GD = 4m	2.6529 kW	3.3132 kW	2.8525 kW	2.9542 kW	3.18103 kW
	GD = 5m	3.7929 kW	3.9349 kW	4.1285 kW	3.6876 kW	3.7444 kW
		H = 8m	H = 12m	H = 16m	H = 20m	H = 24m
	GD = 3m	4.3623 kW	2.7149 kW	2.9556 kW	2.9001 kW	2.8555 kW
GW = 2m	GD = 4m	9.6812 kW	8.0777 kW	6.7666 kW	6.7666 kW	7.0848 kW
	GD = 5m	10.245 kW	12.6364 kW	12.0224 kW	12.2442 kW	11.3658 kW

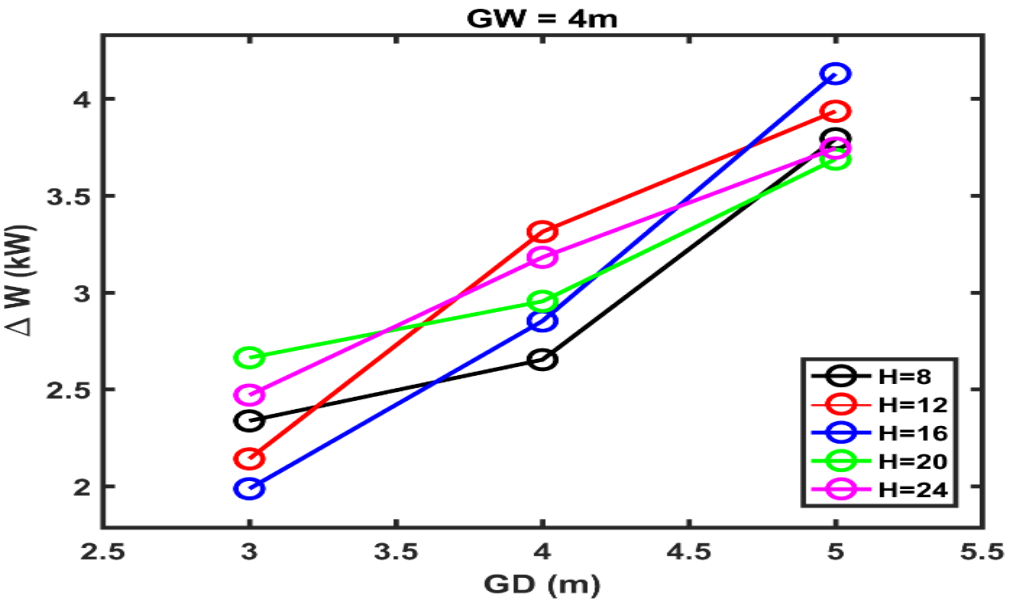

Figure 20: Line Plot of ΔW on GD for GW=4m case, as obtained in MATLAB.

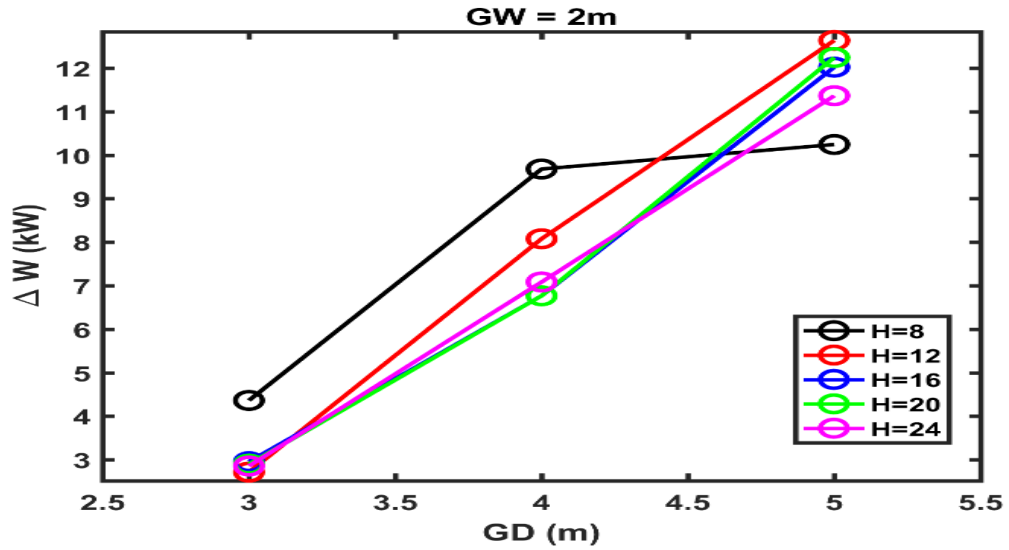

Figure 21: Line Plot of ΔW on GD for GW=2m case, as obtained in MATLAB.

Dependence of Turbulence Intensity on Building Heights

From the plots, it can be interpreted that with an increase in building height, there is an increase in turbulence intensity. And this can be explained if we treat wind flowing in CFD

domain as the wind flowing in a largely closed domain with the building as an obstruction, as mentioned earlier. So, with higher obstruction length, greater turbulence intensity is produced. Since, $Re = \frac{\rho * v * d}{\mu}$ i.e. Re is directly proportional to d (obstruction length in this case). Thus, higher the building (d), higher the Reynolds Number (Re). And higher Reynolds Number implies higher turbulence.

Table 3: Variation of Turbulence Intensity with Design Parameters:

		GD = 3m	GD = 4m	GD = 5m
	H = 8m	0.007489	0.007251	0.007201
	H = 12m	0.1035	0.007116	0.05496
GW = 4m	H = 16m	0.1676	0.1732	0.155
	H = 20m	0.1765	0.1843	0.1738
	H = 24m	0.1804	0.1744	0.1704
		GD = 3m	GD = 4m	GD = 5m
	H = 8m	0.007989	0.002783	0.001838
	H = 12m	0.06307	0.01672	0.01681
GW = 2m	H = 16m	0.154	0.1362	0.09146
	H = 20m	0.2257	0.1978	0.2069
	H = 24m	0.2142	0.2191	0.2396

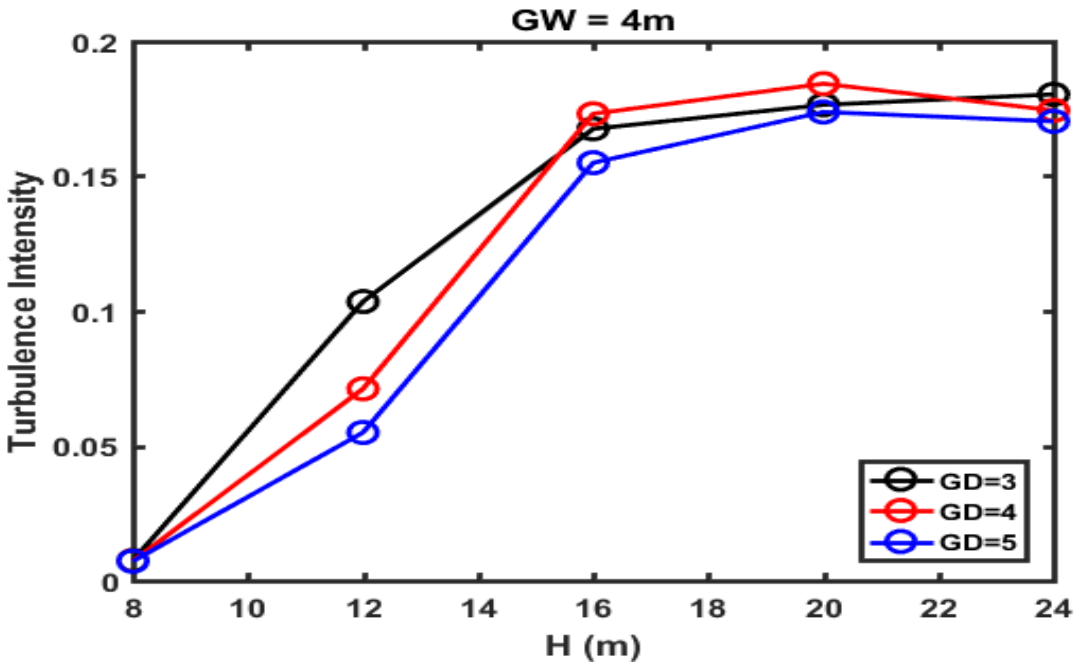

Figure 22: Line Plot of Turbulence Intensity with Height for GW = 4m case, as obtained in MATLAB.

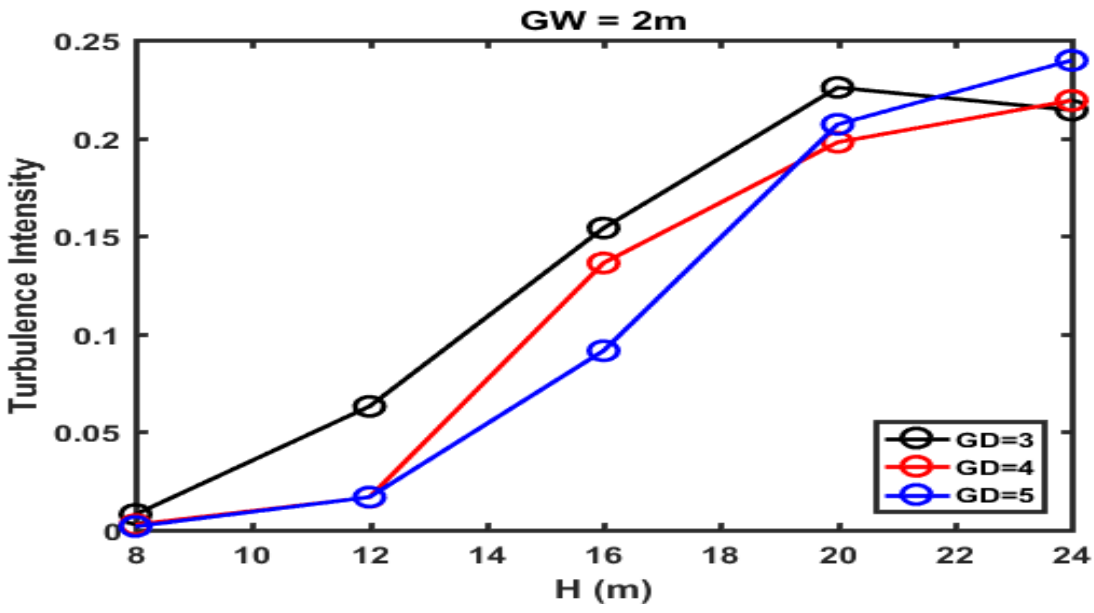

Figure 23: Line Plot of Turbulence Intensity with Height for GW = 2m case, as obtained in MATLAB.

All in all, these statements can't be treated verbatim. This is because the wind flow across the building is like an open system with wind flowing over the building, side of the building and into it through the building gap. Thus, the net effect due to all these actions collectively decides if the velocity is increasing or decreasing due to change in geometrical parameters like H, GD, and GW.

Location of Wind Turbine

From all the cases mentioned above, the most favorable position of installing a wind turbine is found out to be inside the rooftop gap depth. It is here that the maximum acceleration ratio and minimal turbulence intensity is obtained. Consequently, the micro-wind turbine should be mounted within 1-3 m above the base of the rooftop. And for cases with GW = 2m, the mounting position should also lie in the plane of the narrowest distance between the two airfoils i.e. at x_3.

Effects due to Impending Velocity

As the impending velocity is changed from 18 m/s to 10 m/s at 144m height, almost same kind of behavior, like all the above cases, is observed for the effect of Gap Depth on acceleration ratio. For changing gap widths, the acceleration ratio plot shows almost the similar trend as the previous cases, except the maximum acceleration ratio value, is found to reduce from around 1.9 to around 1.7.

Similarly, while analyzing the gain in wind potential, same nature of the line plots are observed but the maximum values are quite less than the one with 18m/s velocity. For

GW=2m, the maximum wind potential gain achieved in 10 m/s case is around 2 kW which is far less as compared to the maximum wind potential gain achieved in 18m/s case i.e. around 12 kW.

Likewise, the effect of building heights on acceleration ratio and wind potential gain is found out to be not that sensitive for both the cases of velocities. However, for 10 m/s case, the effect of building heights on turbulence intensity ratio is found out to be first increasing with height and then decreasing after H = 16m. This anomaly can be explained by the reasoning discussed earlier that the net effect of wind flowing across the building actually decides the behavior of acceleration ratio, wind potential gain or turbulence intensity. If more wind flows inside the roof-top gap opposing the wind flow over the building, it might reduce the velocity magnitude of the wind flow. It is very difficult indeed to interpret or predict any results based on just these observations as the turbulent wind flow across the building needs proper tools to study in detail.

Comparative Numerical Analysis With and Without Turbine

After calculating the ideal location for mounting wind turbine at the building rooftop, CFD modeling is performed for the same old domain but with static wind turbine installed at the ideal location. Average wind velocity in front of the turbine location is measured down for both the cases: with and without the turbine. Contour Plots are also obtained along with the drag and lift force calculations due to the presence of the turbine.

In presence of turbine, the averaged wind velocity just in front of the turbine location is found out to be 25.6324 m/s, generating a wind potential of about 8.993 kW (refer Eq.1). The contour plots of the same are obtained as below:

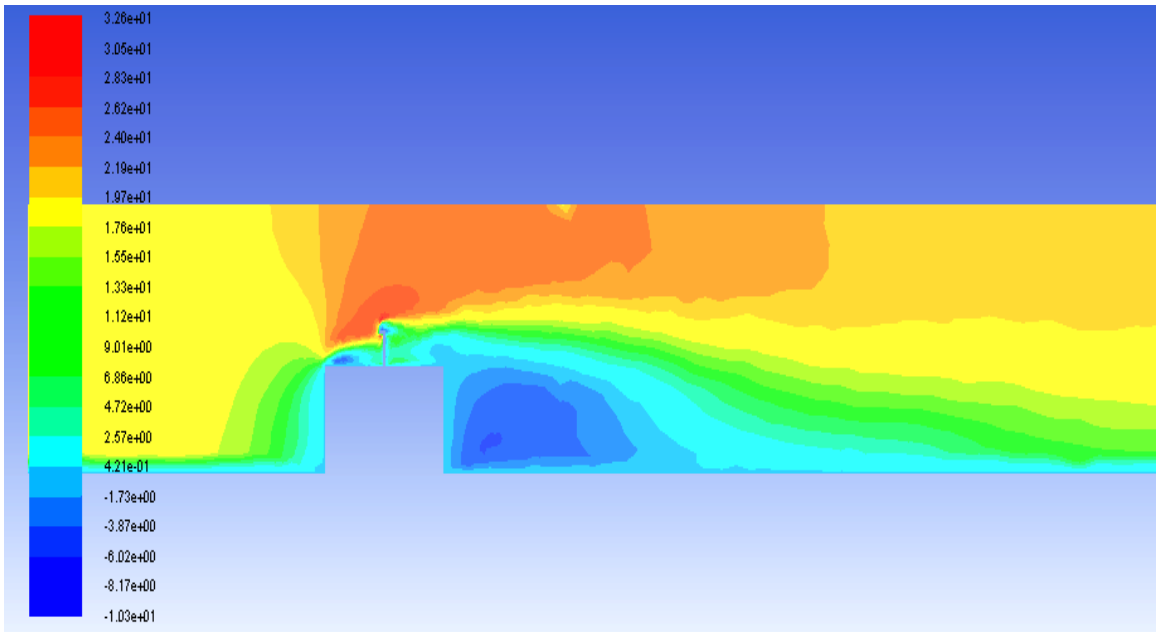

Figure 24: Velocity Contour Plot at mid-plane of domain thickness

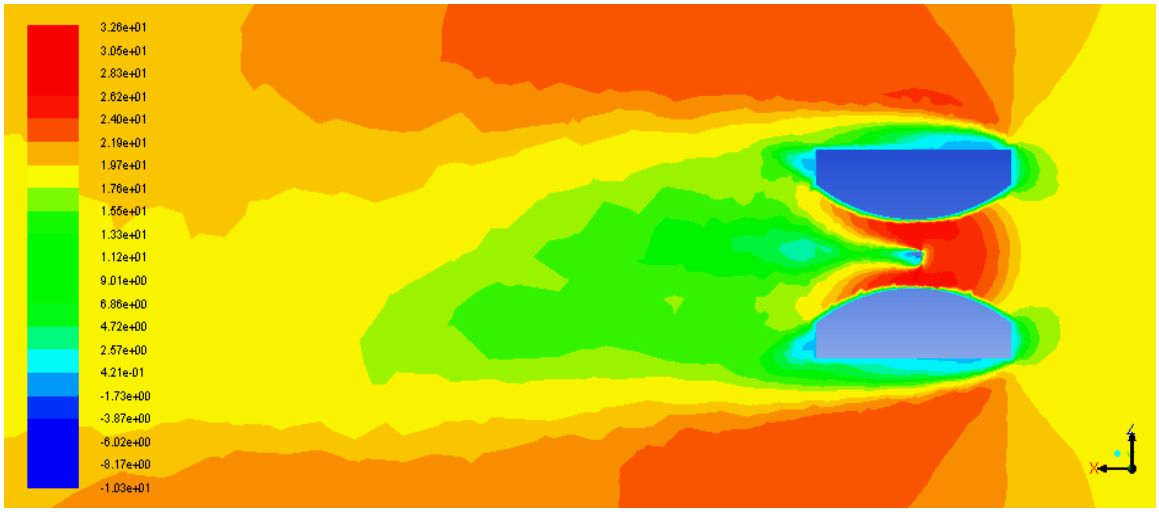

Figure 25: Velocity Contour Plot at half the Gap-Depth

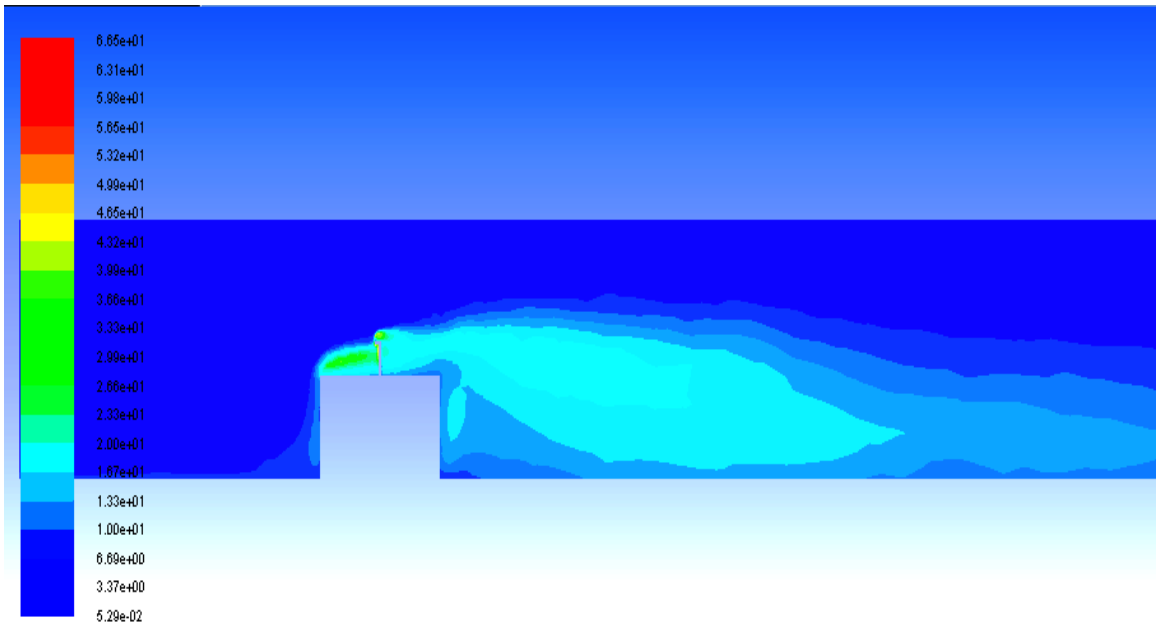

Figure 26: Turbulence Intensity Plot at mid-plane of domain thickness

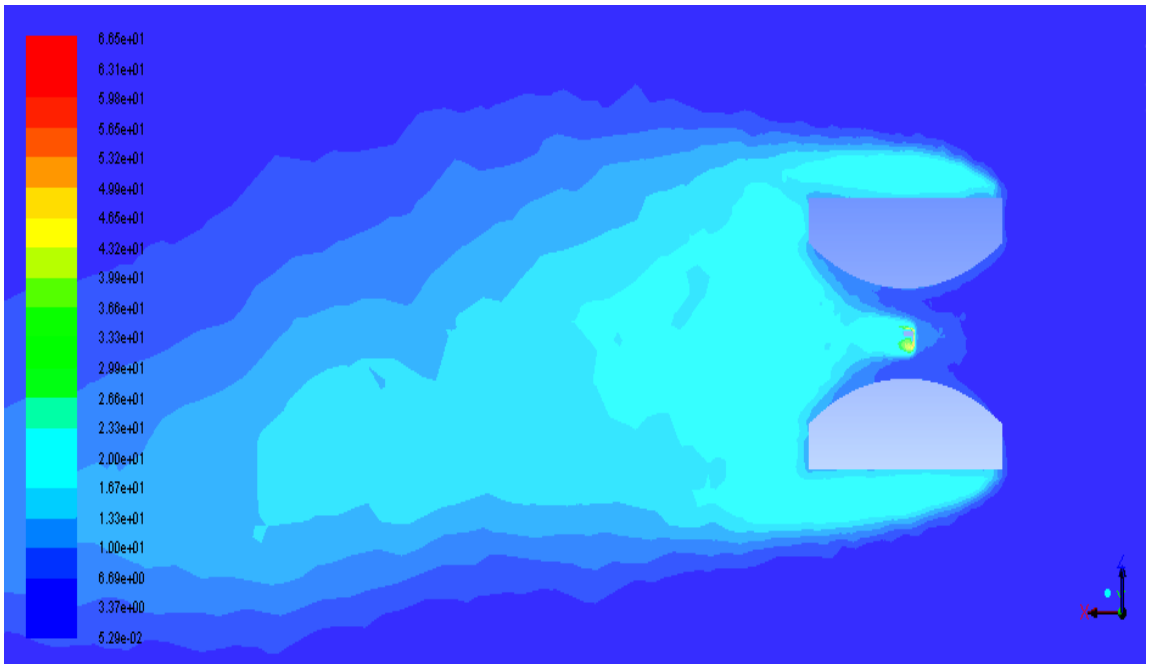

Figure 27: Turbulence Intensity Plot at half gap-depth

The averaged wind velocity in front of the turbine seems reasonable enough for the turbine to be mounted there. Also, the low turbulence intensity of around 10-20% does push the stability conditions in favor of the turbine, which needs to be mounted at such an ideal position.

The net drag and lift forces play a vital role as the aerodynamic forces are quintessential in governing the working of the wind turbine. These forces may also help in rotating the turbine blades. The force in the direction of airflow as the wind pushes against the blade surfaces is called drag. While the force perpendicular to the direction of airflow, generated due to airfoil shaped blades creating a pressure difference between the upper and bottom surfaces is called the lift. These forces are computed numerically in ANSYS Fluent as shown below:

```
Forces

                        Forces (n)
Zone                    Pressure                                    Viscous
turbine                 (400.41577 18.67289 -4.9653931)             (2.2072544 0.0031326711 0.063933536)
----------------------- ------------------------------------------- ------------------------------------------
Net                     (400.41577 18.67289 -4.9653931)             (2.2072544 0.0031326711 0.063933536)

Forces - Direction Vector (1 0 0)
                        Forces (n)                                    Coefficients
Zone                    Pressure       Viscous        Total           Pressure       Viscous         Total
turbine                 400.41577      2.2072544      402.62303       0.34551822     0.0019046368    0.34742286
----------------------- -------------- -------------- --------------- -------------- --------------- ------------
Net                     400.41577      2.2072544      402.62303       0.34551822     0.0019046368    0.34742286
```

Figure 28: Drag Force Calculations in Fluent

The drag forces due to the presence of turbine blades are calculated to be around 402.623 N with a drag coefficient of 0.3474.

```
   599  2.0143e-02  9.9175e-04  5.0557e-04  5.8326e-04  5.6913e-03  1.9589e-03  0:00:01    1

 turbulent viscosity limited to viscosity ratio of 1.000000e+05 in 7095 cells
   600  2.0757e-02  1.0062e-03  5.1578e-04  5.9446e-04  5.7910e-03  1.9805e-03  0:00:00    0

Forces
                         Forces (n)
Zone                     Pressure                                  Viscous
turbine                  (400.41577 18.67289 -4.9653931)           (2.2072544 0.0031326711 0.063933536)
------------------------ ----------------------------------------- -----------------------------------------
Net                      (400.41577 18.67289 -4.9653931)           (2.2072544 0.0031326711 0.063933536)

Forces - Direction Vector (0 1 0)
                         Forces (n)                                  Coefficients
Zone                     Pressure        Viscous         Total       Pressure        Viscous         Total
turbine                  18.67289        0.0031326711    18.676022   0.016112811     2.7031776e-06   0.016115514
------------------------ --------------- --------------- ----------- --------------- --------------- ------------
Net                      18.67289        0.0031326711    18.676022   0.016112811     2.7031776e-06   0.016115514
```

Figure 29: Lift Force Calculations as done in Fluent.

Whereas the lift forces due to the presence of turbine blades are calculated to be around 18.676 N with a lift coefficient of 0.01612.

These values of lift and drag coefficients seem reasonable enough from the aerodynamic point of view.

Moreover, in the absence of the wind turbine, the averaged wind velocity at the same location is found out to be around 26.62 m/s, generating a wind potential of about 10.0768 kW (from Eq.1).

Comparing these two cases, around 25.6324 m/s velocity is achieved for the case involving the presence of turbine which is almost same and close to 26.63 m/s velocity for the case involving no turbine. They are considered almost equivalent. A more detailed study needs to be performed, like including a case with actually rotating wind turbine, in order to study the comparison perfectly.

CHAPTER 6

CONCLUSIONS

The present study reflects the results of CFD Analysis of Wind Power Potential across rooftop gaps of tall buildings. A parametric analysis is carried out to learn the effects of the geometric parameters on acceleration ratio, wind potential gain, and turbulence Intensity. Validation is achieved with the help of Literature review. From the CFD analysis, it is inferred that narrowing the rooftop gap or increasing the depth of the gap favors high wind potential gain by the wind turbine. These geometric parameters governing the aerodynamics of the building shape also play a vital role in mounting micro-wind turbine on roof-tops. However, the present building design is itself very specific and can accommodate mounting of only a single micro wind-turbine. Multiple turbines installation needs a different building design model which can be done in future work. The optimal location of a wind turbine is found out to be around 1 – 3m above the base of the rooftop and inside the gap. Again, these results might vary by taking into account both the wind flow over the building rooftop and through the building gap. Turbulence Intensity is noted to increase with an increase in building height. But, the nature of turbulence intensity needs more research tools to run a detailed analysis and check on its behavior.

Testability of the optimum location of a wind turbine is numerically checked by running another set of simulations for the same domain but in the presence of wind turbine mounted at the favorable position at rooftop gap. It is then compared with another similar computational run but in absence of turbine. From these results, it is concluded that almost

same averaged wind velocity is obtained along with low turbulence intensity around the turbine mounting, in both the cases. These conditions certainly approve the optimum wind potential generation conditions and great stability conditions for installing wind turbines. Also, the drag and lift forces due to the presence of static turbine were calculated and can be used for future studies in detail.

Along with this, future recommendations are also stated to be carried out so as to learn the nuances of building design in affecting the wind power potential. A primary recommendation is made to explore the turbulence intensity parameter in detail by using extensive research tools. Another plausible recommendation made is to conduct another set of numerical simulations for a case involving a rotating micro-turbine mounted on the building rooftop so as to fetch better results in studying the presence of micro-wind turbine in the existing CFD model. Lastly, a final recommendation is made to put up a validation of the existing CFD results which can be achieved experimentally. Conducting wind tunnel test using a 3D printed model of the present building design is highly encouraged for future studies. Ensuring coherence and consistence between the present CFD results and the recommended experimental results can make the present investigation highly valuable.

REFERENCES

Abohela, Hamza, Dudek. 2012.” Effect of roof shape, wind direction, building height and urban configuration on the energy yield and positioning of roof mounted wind turbines”. Renewable Energy 50(2013) 1106-1118.

Application Note TSI-141, 2012. “Turbulence Intensity Measurements Applicable Instrument Models: 9555,9565, 7565, 7575, TA460, TA465, EBT730, PH730, 8715”.

Blocken, Stathopoulos, Carmeliet, Hensen. 2009.”Application of CFD in building performance simulation for the outdoor environment”. Eleventh International IBPSA Conference, Glasgow, Scotland.

Lu, Ip. 2007.” Investigation on the feasibility and enhancement methods of wind power utilization in high-rise buildings of Hong Kong”. Science Direct, Renewable and Sustainable Energy Reviews 13(2009) 450-461.

Sari, Cho. 2014. “CFD and Wind tunnel Analysis for a mounted wind turbine in a tall building for power generation.” Mechatronics, Electrical Power, and Vehicular Technology 05 (2014) 45-50.

Science Direct, Ishugah, Li, Wang, Kiplagat, 2014.”Advances in wind energy resource exploitation in an urban environment: A review.” Renewable and Sustainable Energy Reviews, Volume 37, Pages 613-626.

Silva, Garcia, Peralta, Navarro, Cruz. 2015.”An empirical–heuristic optimization of the building roof geometry for urban wind energy exploitation on high-rise buildings”. Science Direct, Applied Energy, Volume 164, Pages 769-794.

Simic, Havelka, Vrhovcak. 2012.”Small Wind Turbines – A unique segment of the wind power market”. Renewable Energy 50 (2013) 1027-1036.

Source: Wikipedia. Wind Profile Power Law.

APPENDIX A

SET UP IN ANSYS FLUENT

ANSYS Fluent is a computational fluid dynamics solver used for modeling fluid flows, turbulence, and heat transfer problems. It uses FVM methodology.

STEP 1: “Designing the Building kept isolated in an urban landscape”. This is done by using the Design Modeler (DM) provided in ANSYS Workbench. Using the drawing tools provided in the Modeler, at first, the scaled down domain is drawn. Then, the building is drawn extruded from the bottom wall. Further, a turbine is also drawn extruded from the base. All dimensions are taken as per the design scale.

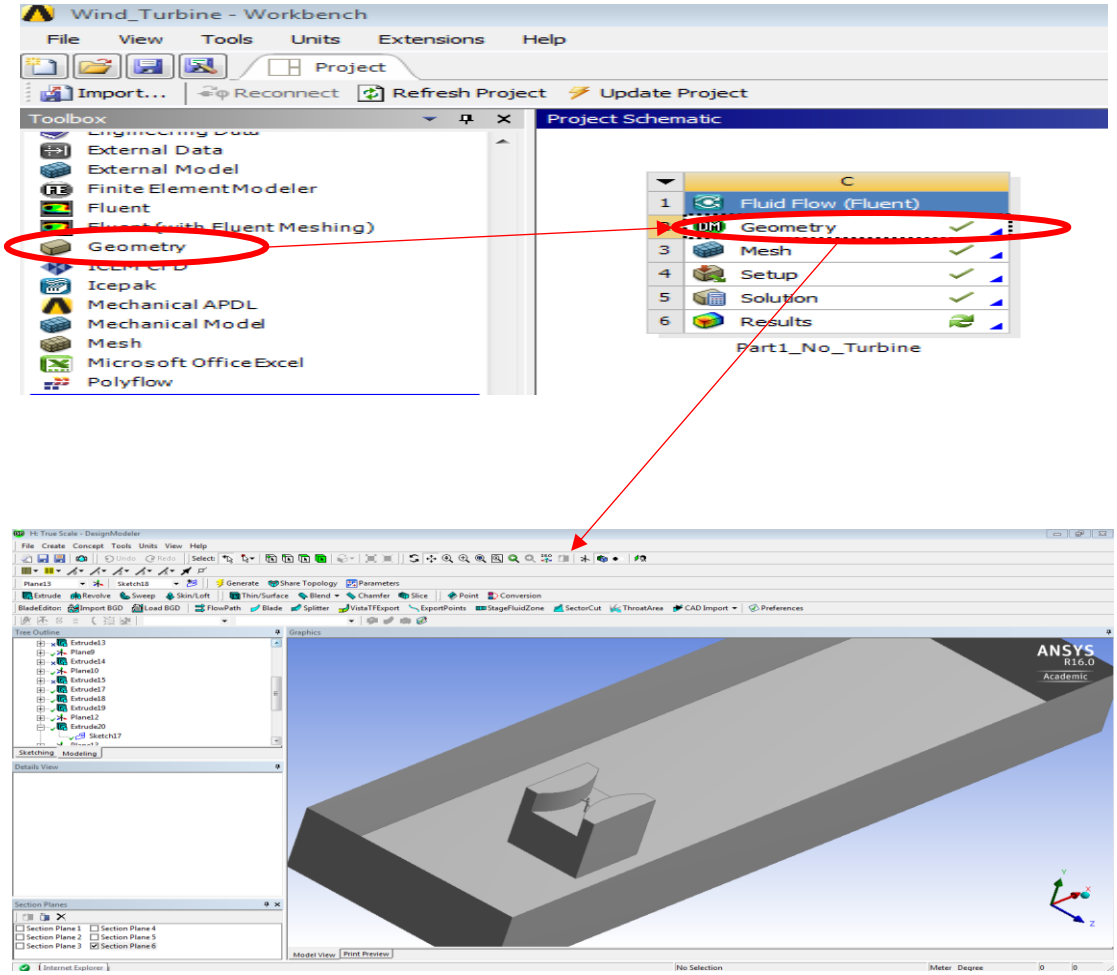

STEP 2: “Meshing the designed model to bring refinement in it.” The Advances Size function is turned “On” for Proximity and Curvature. This results in the generation of a good initial mesh, creating defaults best suited to CFD Solver. Face sizing is implemented on the domain boundaries along with mesh refinement imposed on the building and turbine extrusions. The refinement scale used is 1. Named selection contains the labeled boundaries i.e. velocity inlet, pressure outlet, symmetry, and wall. Mesh quality is verified by using element-wise Mesh metric under Statistics.

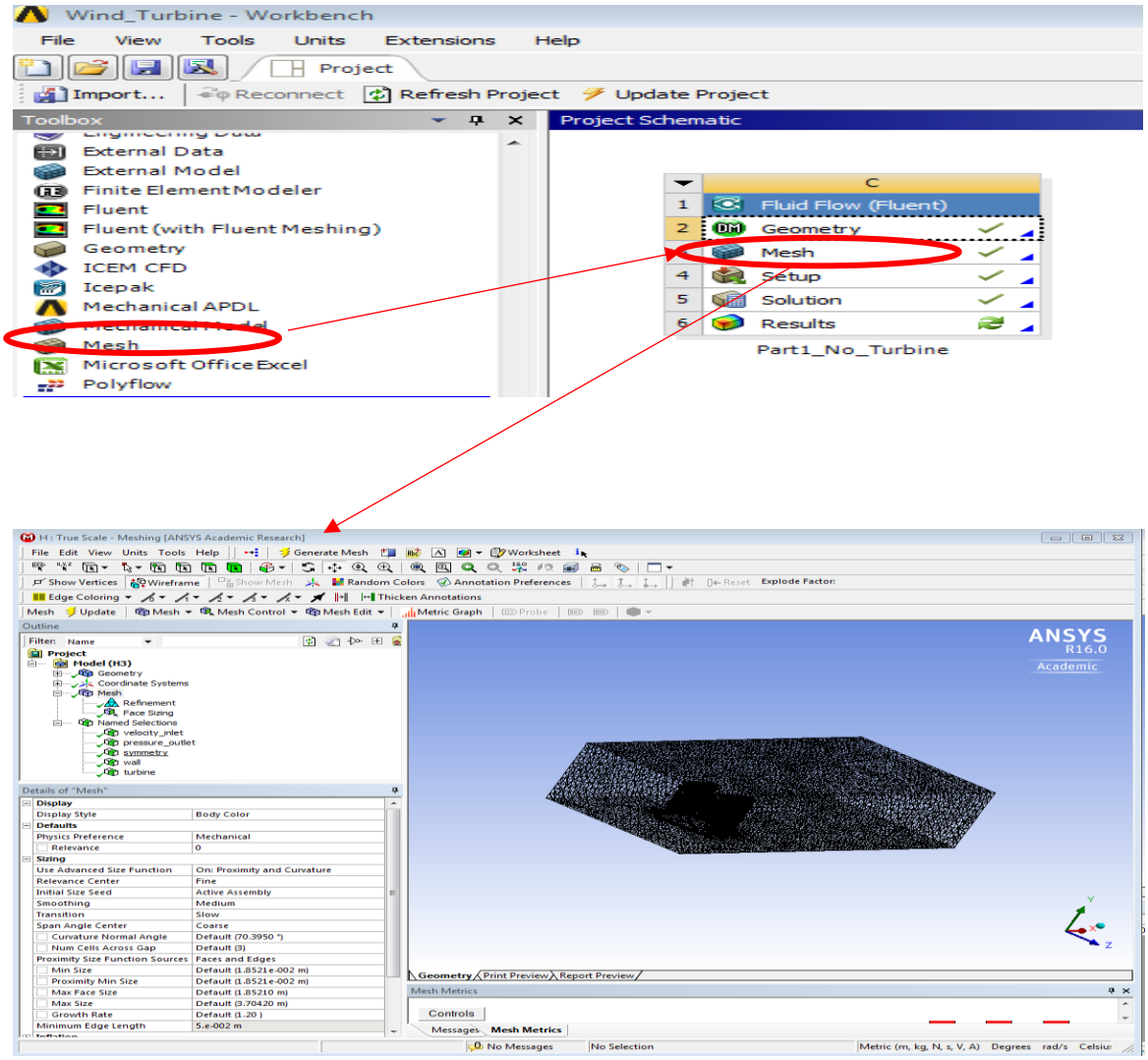

STEP 3: “Running ANSYS Fluent Setup for numerical solution”. After creation of the meshed model, the simulations are then carried out in ANSYS setup which by default programs on imported meshed model. A general setup, favoring a pressure based, steady state and k-ε turbulence model is selected. Following this, boundary conditions are inputted with UDF for inlet velocity and default values for rest of the boundaries. For calculating drag and lift forces on the turbine, reference values are set to be computed from velocity inlet with reference area taken as the projected area of the front side of the turbine. SIMPLEC Scheme with pressure control set at 0.9 or SIMPLE scheme with default solution control values is chosen. The 2^{nd} order in Pressure, Momentum and TKE/TDR is considered. Lift and Drag monitors are created. And a standard solution is then actually run, converging within 600-800 iterations.

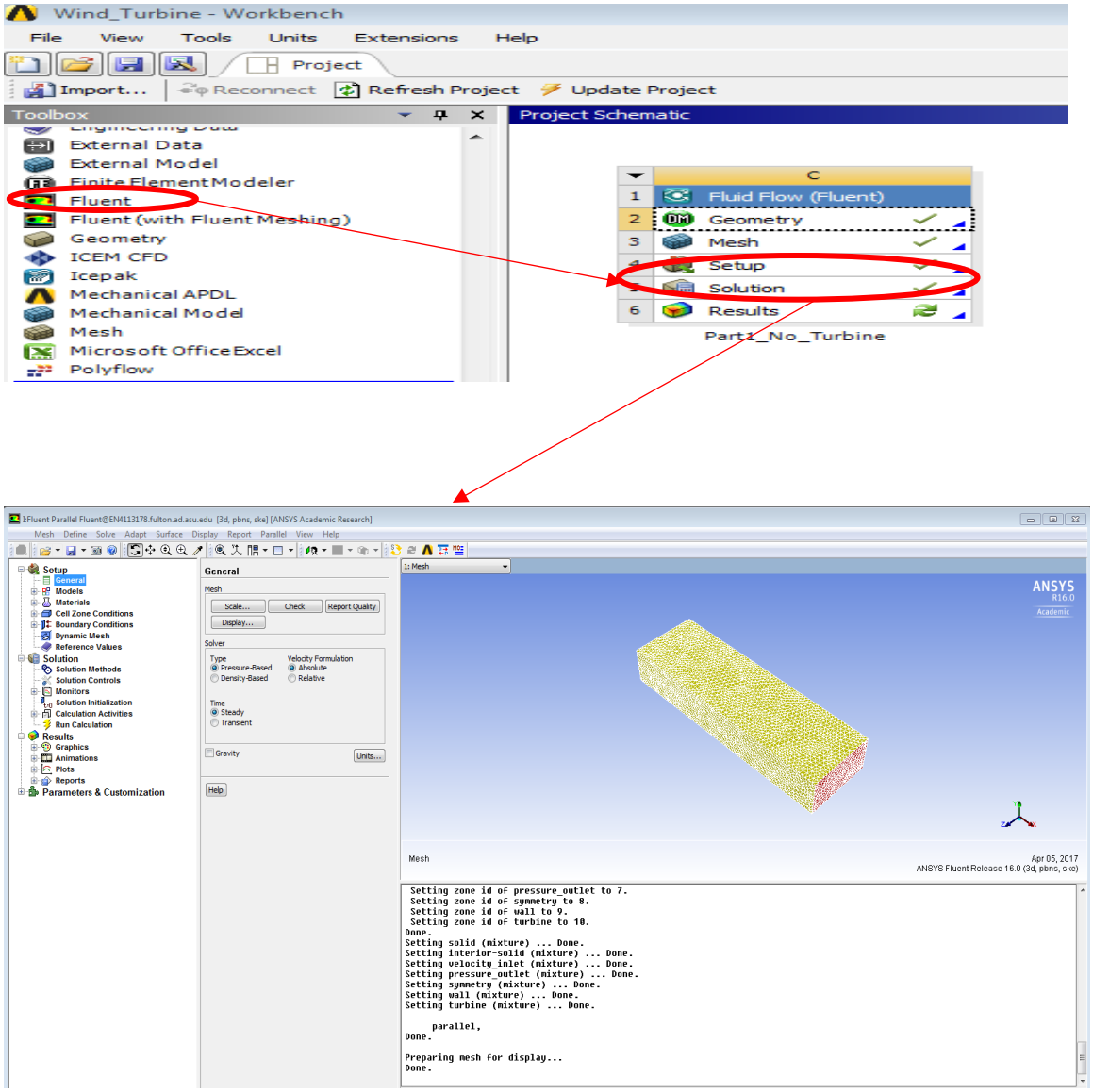

STEP 4: "Post-Processing the results and data from Solution". After running the simulations, the results are obtained using Contour option in the Setup. The desired contours of velocity and turbulence intensity are obtained. Post-processing can also be done in the Results component of ANSYS. Data like wind velocity and turbulence intensity is then extracted along vertical lines in the domain. The data is then imported to MATLAB

as ".dat file" and then processed using MATLAB Coding. The line plots of acceleration ratio and wind potential are then computed from this processed data.

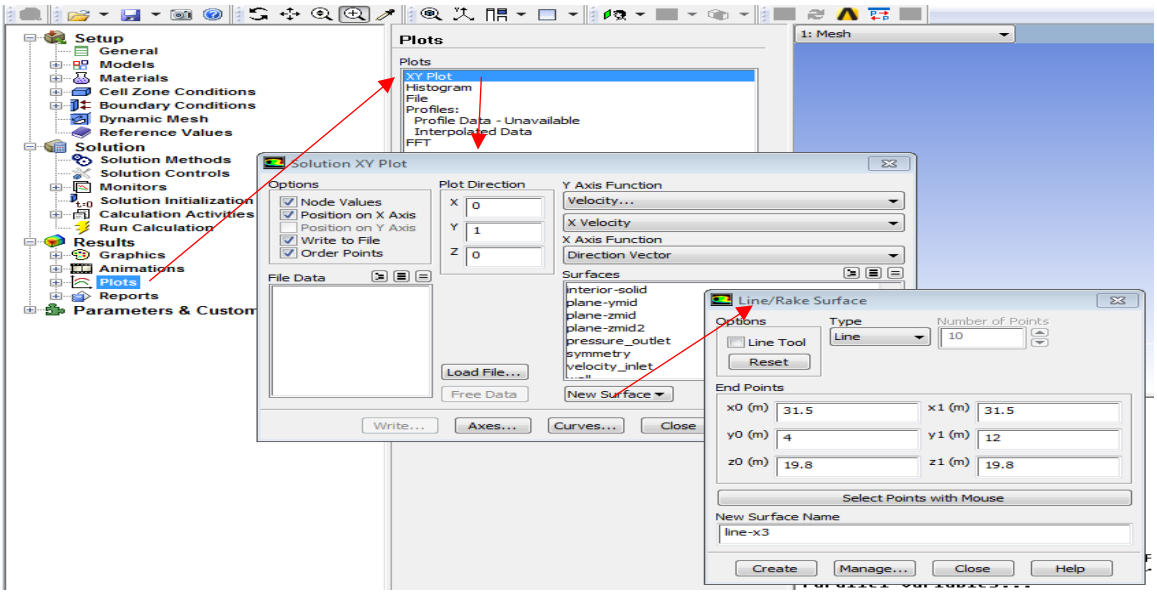

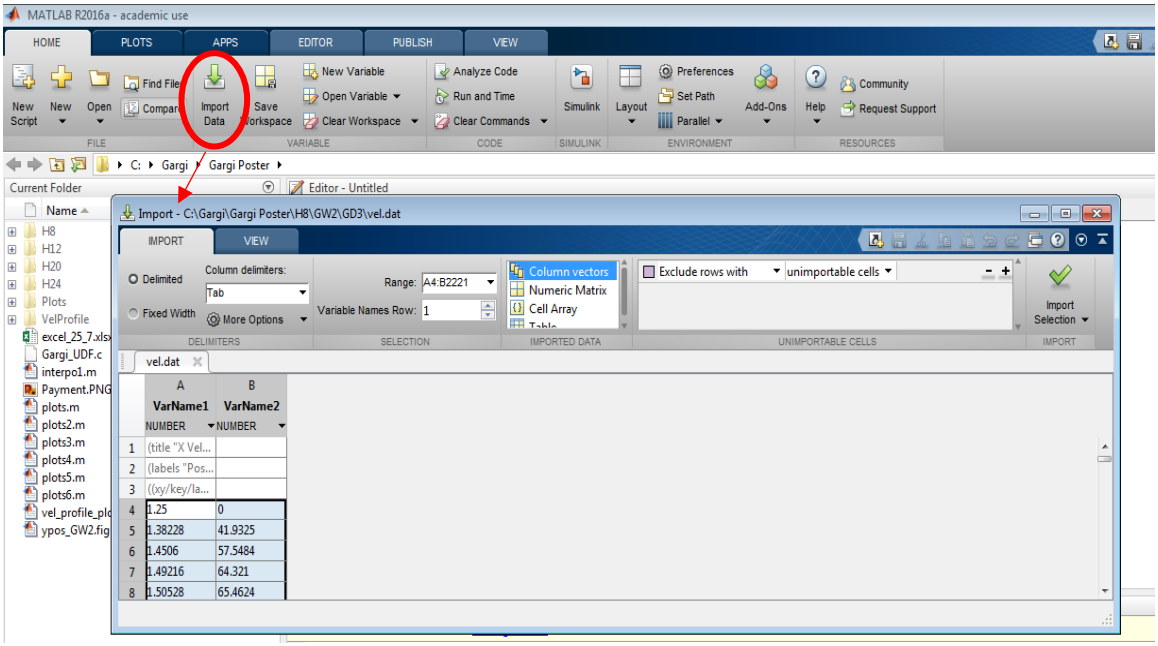

APPENDIX B

USER DEFINED FUNCTION FOR INLET VELOCITY PROFILE

```
#include "udf.h"
DEFINE_PROFILE(inlet_x_velocity,thread,position)



{    float x[nd_nd];
     float y;
     face_t f;


  begin_f_loop(f,thread)
{
    F_CENTROID(x,f,thread);
    y=x[1];
    F_PROFILE(f,thread,position)=72.0*pow(y/144.0,1/7);
}
end_f_loop(f, thread)
}
```

APPENDIX C

CALCULATING ACCELERATION RATIOS USING MATLAB CODING

```
%Plotting Acceleration ratios
 %%%%   WITh BUILDING  %%%%%%%
%Put Values for varying gap depth (line start)
start=3.75;
finish=15;
height=5;
% VarName1=titleXVelocity;
% VarName1=titleTurbulentIntensity;
% VarName3=titleXVelocity1;
% VarName3=titleTurbulentIntensity1;
%Assignment of Variables
% VarName1=Altitude1;
% VarName2=Velocity1;
% VarName3=Altitude2;
% VarName4=Velocity2;
%Segregating y and v
p=0;
for i=1:length(VarName1)
   if (VarName1(i)==finish)
       p=p+1;
       if(p==1)
          for(j=1:i)
          y1(j)=VarName1(j);
```

```
    v1(j)=VarName2(j);
    end
end
if(p==2)
    t=1;
    v2=0;
    for(j=length(y1)+1:i)
    y2(t)=VarName1(j);
    v2(t)=VarName2(j);
    t=t+1;
    end
end
if(p==3)
    t=1;
    v3=0;
    for(j=length(y1)+length(y2)+1:i)
        y3(t)=VarName1(j);
        v3(t)=VarName2(j);
        t=t+1;
    end
end
if(p==4)
    t=1;
```

```
        v4=0;
        for(j=length(y1)+length(y2)+length(y3)+1:i)
            y4(t)=VarName1(j);
            v4(t)=VarName2(j);
            t=t+1;
        end
    end
    if(p==5)
        t=1;
        v5=0;
        for(j=length(y1)+length(y2)+length(y3)+length(y4)+1:i)
            y5(t)=VarName1(j);
            v5(t)=VarName2(j);
            t=t+1;
        end
    end
for(j=length(y1)+length(y2)+length(y3)+length(y4)+length(y5)+length(y6)+1:i)
for(j=length(y1)+length(y2)+length(y3)+length(y4)+length(y5)+length(y6)+length(y7)+1
:i)
for(j=length(y1)+length(y2)+length(y3)+length(y4)+length(y5)+length(y6)+length(y7)+l
ength(y8)+1:i)
  end
end
```

```
%Check lengths
if(length(VarName1)==length(y1)+length(y2)+length(y3)+length(y4)+length(y5))%+len
gth(y6)+length(y7)+length(y8)+length(y9))
   check=1;
else
   check=0;
end

%Putting in an array
y=[y1,y2,y3,y4,y5];%,y6,y7,y8,y9];
v=[v1,v2,v3,v4,v5];%,v6,v7,v8,v9];

%Calculating Differentials
delta_y1=diff(y1);
delta_y2=diff(y2);
delta_y3=diff(y3);
delta_y4=diff(y4);
delta_y5=diff(y5);

y1n=y1;
y2n=y2;
y3n=y3;
```

```
y4n=y4;
y5n=y5;

v1n=v1;
v2n=v2;
v3n=v3;
v4n=v4;
v5n=v5;

%Checking if array is rightly placed or not
for i=1:length(y1)
   if(y(i)==y1(i) && v(i)==v1(i))
      check1=1;
   else
      check1=0;
   end
end
for i=1:length(y2)
   if(y(length(y1)+i)==y2(i) && v(length(v1)+i)==v2(i))
      check2=1;
   else
      check2=0;
   end
```

```
end
for i=1:length(y3)
   if(y(length(y1)+length(y2)+i)==y3(i) && v(length(v1)+length(v2)+i)==v3(i))
      check3=1;
   else
      check3=0;
   end
end
for i=1:length(y4)
   if(y(length(y1)+length(y2)+length(y3)+i)==y4(i)                    &&
v(length(v1)+length(v2)+length(v3)+i)==v4(i))
      check4=1;
   else
      check4=0;
   end
end
for i=1:length(y5)
   if(y(length(y1)+length(y2)+length(y3)+length(y4)+i)==y5(i)         &&
v(length(v1)+length(v2)+length(v3)+length(v4)+i)==v5(i))
      check5=1;
   else
      check5=0;
   end
```

```
end
if(y(length(y1)+length(y2)+length(y3)+length(y4)+length(y5)+length(y6)+length(y7)+le
ngth(y8)+i)==y9(i)                                                    &&
v(length(v1)+length(v2)+length(v3)+length(v4)+length(v5)+length(v6)+length(v7)+lengt
h(v8)+i)==v9(i))

%Monotonic increase
flag1=0;
flag2=0;
flag3=0;
flag4=0;
flag5=0;

p1=0;p2=0;p3=0;p4=0;p5=0;
j=1;
for i=1:length(y1)-1
   if(delta_y1(i)==0)
      p1(j)=i;
      flag1=1;
      j=j+1;
   end

end
```

```
if(flag1==1)
y1n(p1)=[];
v1n(p1)=[];
end
j=1;
for i=1:length(y2)-1
   if(delta_y2(i)==0)
      p2(j)=i;
      flag2=1;
      j=j+1;
   end
end
if(flag2==1)
y2n(p2)=[];
v2n(p2)=[];
end
j=1;
for i=1:length(y3)-1
   if(delta_y3(i)==0)
      p3(j)=i;
      flag3=1;
      j=j+1;
   end
```

```
end
if(flag3==1)
y3n(p3)=[];
v3n(p3)=[];
end
j=1;
p4=0;
for i=1:length(y4)-1
   if(delta_y4(i)==0)
      p4(j)=i;
      flag4=1;
      j=j+1;
   end
end
if(flag4==1)
y4n(p4)=[];
v4n(p4)=[];
end
j=1;
for i=1:length(y5)-1
   if(delta_y5(i)==0)
      p5(j)=i;
      flag5=1;
```

```
      j=j+1;
    end
end
if(flag5==1)
y5n(p5)=[];
v5n(p5)=[];
end

%Strictly increasing
 increase1=all(diff(y1n)>0);
 increase2=all(diff(y2n)>0);
 increase3=all(diff(y3n)>0);
 increase4=all(diff(y4n)>0);
 increase5=all(diff(y5n)>0);

%Interpolating velocity according to the height
y1i=start:0.1:y1n(length(y1n));
v1i=interp1(y1n,v1n,y1i);

y2i=start:0.1:y2n(length(y2n));
v2i=interp1(y2n,v2n,y2i);

y3i=start:0.1:y3n(length(y3n));
```

```
v3i=interp1(y3n,v3n,y3i);

y4i=start:0.1:y4n(length(y4n));
v4i=interp1(y4n,v4n,y4i);

y5i=start:0.1:y5n(length(y5n));
v5i=interp1(y5n,v5n,y5i);

%%%%   WITHOUT BUILDING  %%%%%%%%%%%%%%%%%%%%
%Segregating y and v
p=0;
for i=1:length(VarName3)
   if (VarName3(i)==finish)
      p=p+1;
      if(p==1)
         for(j=1:i)
            y1e(j)=VarName3(j);
            v1e(j)=VarName4(j);
         end
      end
      if(p==2)
         t=1;
         v2e=0;
```

```
    for(j=length(y1e)+1:i)
    y2e(t)=VarName3(j);
    v2e(t)=VarName4(j);
    t=t+1;
    end
end
if(p==3)
    t=1;
    v3e=0;
    for(j=length(y1e)+length(y2e)+1:i)
        y3e(t)=VarName3(j);
        v3e(t)=VarName4(j);
        t=t+1;
    end
end
if(p==4)
    t=1;
    v4e=0;
    for(j=length(y1e)+length(y2e)+length(y3e)+1:i)
        y4e(t)=VarName3(j);
        v4e(t)=VarName4(j);
        t=t+1;
    end
```

```
        end
        if(p==5)
            t=1;
            v5e=0;
            for(j=length(y1e)+length(y2e)+length(y3e)+length(y4e)+1:i)
                y5e(t)=VarName3(j);
                v5e(t)=VarName4(j);
                t=t+1;
            end
        end
    end
end

%Check lengths
if(length(VarName3)==length(y1e)+length(y2e)+length(y3e)+length(y4e)+length(y5e))
checke=1;
else
    checke=0;
end

%Putting in an array
ye=[y1e,y2e,y3e,y4e,y5e];
ve=[v1e,v2e,v3e,v4e,v5e];
```

```
%Checking if array is rightly placed or not
for i=1:length(y1e)
   if(ye(i)==y1e(i) && ve(i)==v1e(i))
      checke1=1;
   else
      checke1=0;
   end
end
for i=1:length(y2e)
   if(ye(length(y1e)+i)==y2e(i) && ve(length(v1e)+i)==v2e(i))
      checke2=1;
   else
      checke2=0;
   end
end
for i=1:length(y3e)
   if(ye(length(y1e)+length(y2e)+i)==y3e(i) && ve(length(v1e)+length(v2e)+i)==v3e(i))
      checke3=1;
   else
      checke3=0;
   end
end
for i=1:length(y4e)
```

```
    if(ye(length(y1e)+length(y2e)+length(y3e)+i)==y4e(i)                    &&
ve(length(v1e)+length(v2e)+length(v3e)+i)==v4e(i))
        checke4=1;
    else
        checke4=0;
    end
end
for i=1:length(y5e)
    if(ye(length(y1e)+length(y2e)+length(y3e)+length(y4e)+i)==y5e(i)        &&
ve(length(v1e)+length(v2e)+length(v3e)+length(v4e)+i)==v5e(i))
        checke5=1;
    else
        checke5=0;
    end
end

%Checking if Strictly increasing or not
 increasee1=all(diff(v1e)>0);
 increasee2=all(diff(v2e)>0);
 increasee3=all(diff(v3e)>0);
 increasee4=all(diff(v4e)>0);
 increasee5=all(diff(v5e)>0);
```

```
%Calculating Theroretical velocity
h=16;
umax=18*4;
v1et=umax*((y1e./h).^(1/7));
v2et=umax*((y2e./h).^(1/7));
v3et=umax*((y3e./h).^(1/7));
v4et=umax*((y4e./h).^(1/7));
v5et=umax*((y5e./h).^(1/7));

%Interolating velocity without building according to the height
y1ie=start:0.1:y1e(length(y1e));
v1ie=interp1(y1e,v1e,y1ie);
v1iet=interp1(y1e,v1et,y1ie);

y2ie=start:0.1:y2e(length(y2e));
v2ie=interp1(y2e,v2e,y2ie);
v2iet=interp1(y2e,v2et,y2ie);

y3ie=start:0.1:y3e(length(y3e));
v3ie=interp1(y3e,v3e,y3ie);
v3iet=interp1(y3e,v3et,y3ie);

y4ie=start:0.1:y4e(length(y4e));
```

```
v4ie=interp1(y4e,v4e,y4ie);

v4iet=interp1(y3e,v4et,y4ie);


y5ie=start:0.1:y5e(length(y5e));

v5ie=interp1(y5e,v5e,y5ie);

v5iet=interp1(y5e,v5et,y5ie);


%Calculating acceleration ratios

a1=v1i;%./v1ie;

a2=v2i;%./v2ie;

a3=v3i;%./v3ie;

a4=v4i;%./v4ie;

a5=v5i;%./v5ie;


%Calculating Theoretical acceleration ratios

a1t=v1i;%./v1iet;

a2t=v2i;%./v2iet;

a3t=v3i;%./v3iet;

a4t=v4i;%./v4iet;

a5t=v5i;%./v5iet;

a=[a1,a2,a3,a4,a5];%,a6,a7,a8,a9];

max_acc=max(a)

min_acc=min(a)
```

```
for i=1:length(a)
   if(a(i)==max_acc)
      pos_max=i;
   end
   if(a(i)==min_acc)
      pos_min=i;
   end
end

line_max=pos_max/length(a1);
line_min=pos_min/length(a1);

%Plotting all (NOTE LEGENDS CHANGE EVERY TIME)
plot(a1,y1ie,'r',a2,y1ie,'b',a3,y1ie,'g',a4,y1ie,'m',a5,y1ie);%,'y',a6,y1ie,'-ro');
legend('x=30','x=30.75','x=31.5','x=32.25','x=33');
%Maximum AR/TIR near building (CENTRELINE - a5/y5) for Micro-Wind Turbine
j=1;

y5range=0;
a5range=0;
for(i=1:length(y5ie))
   if(y5ie(i)<=height+3)
      y5range(j)= y5ie(i);
```

```
      a5range(j)=a5(i);
      j=j+1;
   end
end
max_centre=max(a5range)
min_centre=min(a5range)
for(i=1:length(a5range))
   if(a5range(i)==max_centre)
   pos_centre_max=i;
   end
   if (a5range(i)==min_centre)
   pos_centre_min=i;
   end
end
```